Analysis of Magnetic Field and Electromagnetic Forces in Transformer and Superconducting Magnets

A THESIS SUBMITTED IN PARTIAL FULFILLMENT OF THE REQUIREMENT FOR THE DEGREE OF

Master of Technology

In

Electrical Engineering

By

Ashish Kumar Patel

Under the guidance of

Dr. S. Gopalakrishna

Department of Electrical Engineering

National Institute of Technology, Rourkela

Rourkela-769008

Analysis of Magnetic Field and Electromagnetic Forces in Transformer and Superconducting Magnets

A THESIS SUBMITTED IN PARTIAL FULFILLMENT OF THE REQUIREMENT FOR THE DEGREE OF

Master of Technology

In

Electrical Engineering

By

Ashish Kumar Patel

Under the guidance of

Dr. S. Gopalakrishna

Department of Electrical Engineering

National Institute of Technology, Rourkela

Rourkela-769008

Dedicated

To

My beloved parents

Department of Electrical Engineering

National Institute of Technology, Rourkela

Certificate

This is to certify that the thesis entitled, "**Analysis of Magnetic Field and Electromagnetic Forces in Transformer and Superconducting Magnets**" submitted by Mr. Ashish Kumar Patel in partial fulfillment of the requirements for the award of **Master of Technology** Degree in **Electrical Engineering** with specialization in "**Power Electronics and Drives**" during session 2013-15 at the National Institute of Technology, Rourkela is an authentic work carried out by him under my supervision and guidance. This work has not been submitted at other University/ Institute for the award of any degree or diploma.

Date: **Dr. S. Gopalakrishna**

Place: Department of Electrical Engineering

National Institute of Technology

Rourkela-769008

Acknowledgement

I would like to express my sincere gratitude to my supervisor Dr. S. Gopalakrishna for his guidance, encouragement, and support throughout the course of this work. It was an invaluable learning experience for me to be one of his students. As my supervisor his insight, observations and suggestions helped me to establish the overall direction of the research and contributed immensely for the success of this work.

I express my gratitude to Prof. A. K. Panda, Head of the Department, Electrical Engineering for his invaluable suggestions and constant encouragement all through this work. My thanks are extended to my colleagues in power control and drives, who built an academic and friendly research environment that made my study at NIT, Rourkela most fruitful and enjoyable. I would also like to acknowledge the entire teaching and non-teaching staff of Electrical department for establishing a working environment and for constructive discussions. Finally, I am always indebted to all my family members, especially my parents, for their endless support and love.

Last but not least I would like to thank my parents, who taught me to work hard by their own example. They provided me much support being apart during the whole tenure of my stay in NIT Rourkela.

ASHISH KUMAR PATEL

ROLL NO. - 213EE4332

Abstract

Superconducting magnets are electromagnets that are wound using coils made of superconducting wires. Due to the ability of superconductors to carry current with no resistance, these magnets are able to produce high magnetic fields with very less power consumption required towards refrigeration only. In this day and age magnet technology happens to be an increasingly critical factor in the progress of science and technology. The ultra-high magnetic field plays a significant part in letting us research and delve into the origins of life and disease prevention, high energy physics experiments, enabling us better understand the world.

Due to the complex structures and stringent requirements the design of magnets now can no longer be accomplished by just simple analytical calculations. To decide and optimize the electromagnetic structure parameters of large scale magnet, high level numerical analysis technologies are being extensively studied. As different problems have distinct aspects viz. field of application, material properties, geometrical features, hence there is not a single process to handle all probable scenarios. Numerical analysis of magnetic field distribution with respect to time and space is being done by obtaining the solution to Maxwell's equation numerically under predefined boundary and initial conditions in addition with all sort of mathematical optimal technologies.

In this thesis, with the use of finite element method (FEM) based software ANSYS Maxwell, study of magnetic field distribution and electromagnetic force distribution for a simple solenoid, notched solenoid magnet design is done. Additionally a magnet design with multiple Coaxial winding sections is simulated using ANSYS Maxwell and magnetic field distribution, radial and axial forces on the windings are studied. A design method, for optimal configuration of multi section superconducting magnets utilizing a modified genetic algorithm is studied. Also a transformer is modelled using Maxwell to study magnetic field distribution and electromagnetic forces and the effect of asymmetry in windings.

Contents

List of figures

List of Symbols

B	Flux density vector
H_c	Critical magnetic field
J_c	Critical current density
T_c	Critical temperature
B_0	Central magnetic field
B_w	Maximum field on the winding
J	Current density vector
F_x	Radial force
F_y	Axial force
NI	Ampere turns
μ_0	Absolute permeability
H_w	Winding height in meters

CHAPTER 1

INTRODUCTION

1.1 Superconductivity

Dutch physicist Heike Kamerlingh Onnes, while studying the resistivity of metals at low temperatures, discovered superconductivity in mercury samples in year 1911. A sharp drop in resistance of mercury samples at around 4.15K to a very small value was observed by Onnes. This phenomenon of near absence of resistance was termed as superconductivity. Since then a lot of metals, alloys and intermetallic compounds have been found to show superconductivity below the individual characteristic temperature of each material also called as the critical temperature, T_c. the variation of resistance of superconducting and non-superconducting material with respect to temperature is shown below in Fig. 1.1. A nonlinear relationship is seen between resistance and temperature.

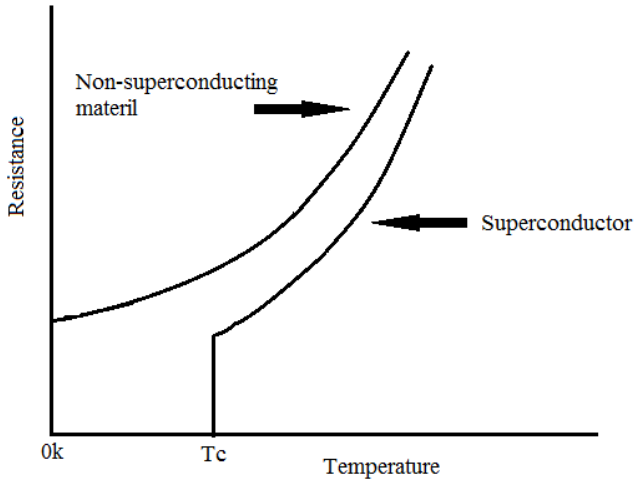

Fig. 1.1 variation in resistance of superconducting and non-superconducting material with temperature

Similarly for a material to observe superconductivity it must be below a specified magnetic field and a specified current density also termed as critical magnetic field (H_c) and critical current density (Ji) respectively. Critical temperature (T_c), critical magnetic field (H_c) and critical current density (J_i), these three parameters create a critical surface for superconducting material as shown in Fig. 1.2. As long as the material is inside this critical surface it exhibits superconducting

properties, but outside this critical surface it loses its superconductivity and behaves as a normal conductor having finite resistance.

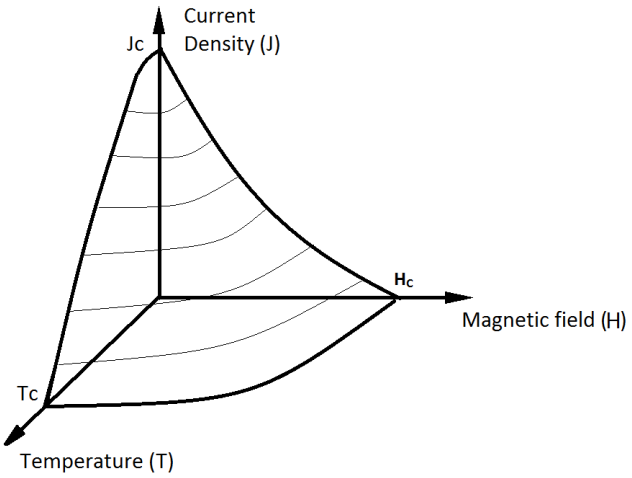

Fig. 1.2 critical surface of a typical superconductor

The critical magnetic field and temperature are intrinsic or inherent properties of material and hence cannot be improved by manufacturing process. On the other hand, critical current can be quite enhanced by various manufacturing process like metallurgical treatments used in the fabrication of the wire.

1.2 Type I and Type II Superconductors

It was discovered by Meissner and Ochsenfeld in the year 1933 that a metal in superconducting state expels the magnetic induction completely when subjected to a magnetic field. This is due to the magnetic field produced by the surface currents, which cancel the applied field inside the superconductor. This fundamental property of material by which it expels the flux from its interior is known as Meissner effect.

Now based on the way the magnetic flux or induction is expelled from the material, superconductors are divided into two groups known as Type I and Type II. In Type I superconductors, up to the critical field (H_c) total magnetic induction expulsion is observed and beyond H_c no expulsion of magnetic induction takes place. Hence Type I super conductor exhibits

perfect diamagnetism in the superconducting state. Magnetization curve for Type I and Type II superconductors are shown in Fig. 1.3.

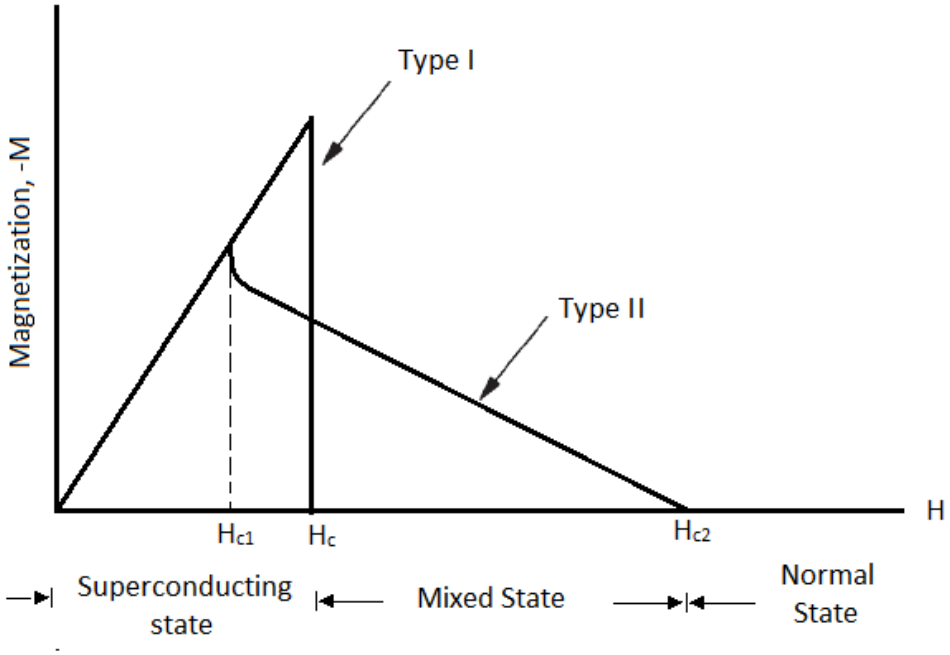

Fig. 1.3 Magnetization curve for typical Type I and Type II superconductors

Type II superconductors, on the other hand have two critical magnetic fields, denoted by H_{c1} and H_{c2} in Fig. 1.3. For applied magnetic field below H_{c1} they behave similar to a Type I material as complete magnetic induction expulsion is observed. For applied magnetic field greater than H_{c2}, complete flux penetration takes place and Type II superconductors are in normal state. Meanwhile for applied magnetic fields between H_{c1} and H_{c2}, the material allows partial flux penetration and is in a mixed state also called as vortex state but still exhibits superconducting properties.

Type II materials have the highest possible critical parameters because they remain superconducting upto H_{c2} which is typically much larger than critical field (H_c) of Type I superconductors, and thus are practical for magnet applications.

1.3 Superconducting Magnets and Applications

Kamerlingh onnes realized the immense technological potential of his discovery of superconductivity, like the creation of superconducting electromagnets. Because these magnets

would be able to produce high magnetic fields with very less power consumption required for refrigeration only, due to the ability of superconductors to carry current with no resistance. However, it was not until year 1960 that construction of practical superconducting electromagnets became possible as a result of the discovery of high-field, high current carrying conductors based on Type II superconductors. These conductors were intermetallic compounds, like niobium-tin (Nb_3Sn) and alloys, like niobium-titanium (NbTi) which often had individual elements not having superconducting properties themselves.

In terms of power consumption, Superconducting magnets are far superior to that of conventional water cooled magnets. For example, a 15T superconducting magnet with a 5cm bore requires only a few hundred watts of operating power compared to the few megawatts of power required by an equivalent copper wound magnet operating at room temperature. Additionally superconducting magnets provide further savings owing to its smaller size and lighter weight compared to those of copper magnets.

Nowadays superconducting magnets find extensive use in several high-field applications. Some of these applications are superconducting magnetic energy storage (SMES), large scale electric motors and generators, magnets for nuclear magnetic resonance, magnets for controlled thermonuclear fusion, magnets for high energy physics research and magnetically levitated vehicles.

1.4 Literature review

The strange yet remarkable property shown by certain metals and alloys of abrupt drop in resistance to zero below a a certain temperature called as critical temperature was termed as superconductivity by Kamerlingh Onnes, subsequent to his discovery of this phenomenon while working on mercury sample in the year 1911. Onnes soon realized the tremendous technical and scientific potential this discovery of his and envisioned large electromagnets with moderate power consumption being able to generate large magnetic fields. But it was not until late 1950s and early 1960s that onnes' vision became a practical prospect with the discovery of Type II superconductors like niobium titanium (NbTi) and niobium tin (Nb_3Sn) [1].

Superconductivity today finds its use in a plethora of fields viz. research magnets, high energy physics, controlled thermonuclear fusion, magnetohydrodynamic power generation, D.C. motors,

A.C. machines, energy storage, magnetic separation and magnetic levitation etc. [1]. The different types of windings used commonly, the magnetic field shapes produced by them and the various methods like numerical methods being used to calculate these fields are explained in [1].

A super conductor magnet consisting of ten coaxial niobium-titanium (NbTi) coils which are connected in series is designed and its field configuration is optimized in order to be able to get a central magnetic field adjustable in the range of 0 to 9.2T which stays uniform over an axial length of approximately 200mm, in order to be able to perform a gamut of gyrotron experiment frequencies [2].

It is established that minimum power homogeneous magnet design can be considered as linear programming problem and subsequently a technique for the purpose of designing homogeneous magnets using linear programing is introduced. It is also shown that this technique is equally applicable to minimum conductor mass superconducting magnet design. One shielded superconducting magnet design and multiple resistive magnet design are provided to further show the flexibility of the technique [5]. A novel method for optimal configuration design, which utilizes a modified genetic algorithm to get minimum winding volume for multi section superconducting magnets is introduced. The algorithm detail and a couple of its application to three section superconducting magnets are shown [4].

1.5 Motivation

The growth and development of superconducting magnet science and technology is reliant on higher magnetic field strength and better field quality. With the advancements in superconducting materials and cryogenic technologies, magnetic field strength of superconducting magnets are increasing. Not only higher magnetic fields can provide technical support for scientific research but also play a significant role to play in medical imaging, industrial production, electrical power, energy storage technology etc. hence the magnetic field is an exciting cutting edge technology fully of prospects and challenges and also essential for significant discoveries in science and technology.

1.6 Objectives

- To design and model a winding design using FEM based software ANSYS Maxwell, so as to get more uniform axial field distribution compared to a simple solenoid winding.
- To model a solenoid with multiple layer of coaxial windings to accomplish a long length uniform axial field adjustable in the range of 0 to 9.2T, while keeping the peak magnetic field inside the coils within its critical surface, Also to calculate hoop stress and axial stress on the windings.
- To model a transformer design using ANSYS Maxwell with a small axial asymmetry introduced between the LV and HV winding and to subsequently study the variation of magnetic field, axial and radial force distribution, end thrust on both LV and HV windings of the transformer.

1.7 Thesis layout

Chapter 1 consists of a brief overview about superconductivity, types of superconductors, superconducting magnets and applications, literature review, objectives and thesis layout.

Chapter 2 describes about different winding configuration and field shapes, modelling of simple and notched solenoid using finite element method (FEM), and an example of optimal design method using genetic algorithm.

Chapter 3 consists of modelling of 9.2T magnet with ten coaxial coils using FEM based ANSYS Maxwell and simulation results of magnetic fields in the magnet and electromagnetic forces on the windings.

Chapter 4 explains about short circuit forces and their effects on transformer windings, modelling of transformer using finite element method (FEM), and calculation of axial forces due to winding asymmetry.

Chapter 5 consists of summary of the work done, future scope of the work, and references.

CHAPTER 2

FIELD SHAPES AND WINDING CONFIGURATIONS

2.1 Magnetic fields in a Simple solenoid

To reduce magnetic reluctance, magnets typically use a soft iron core. The number of ampere turns required and the corresponding power consumption is minimized as a result of reduction in the reluctance. Meanwhile superconducting magnets are not restricted by this, as additional ampere turns needed are relatively cheaper and hence do not increase the refrigeration power load significantly. Due to this reason iron cores are very rarely used to increase the working field in superconducting solenoid, but are often used for shielding that is to reduce stray fields. And hence, in this case a simple iron core free calculation of magnetic field distribution in the solenoid will be sufficient.

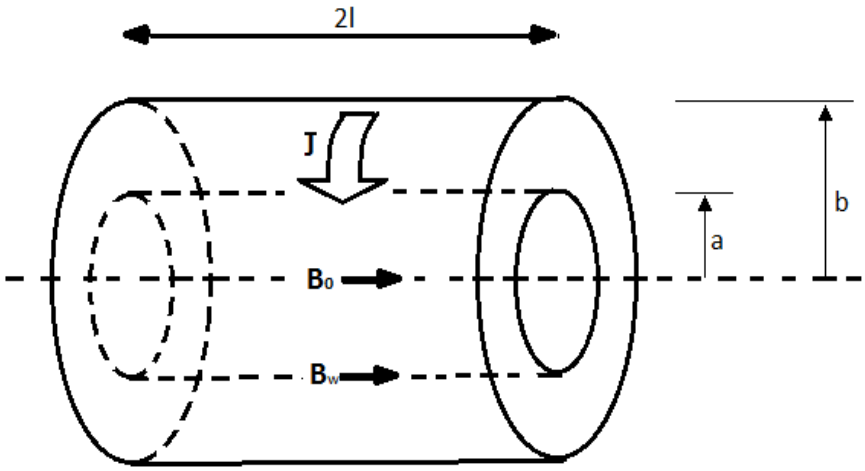

Fig. 2.1 A simple solenoid winding

By integrating the magnetic field by individual current carrying filaments the magnetic field at center can be expressed as follows

$$B_0 = Ja\mathrm{F}(\alpha\beta) \tag{1}$$

Where

$$\mathrm{F}(\alpha\beta) = \mu_0\beta \ln\left\{\frac{\alpha + (\alpha^2+\beta^2)^{\frac{1}{2}}}{1 + (1+\beta^2)^{\frac{1}{2}}}\right\} \tag{2}$$

$$\alpha = b/a \tag{3}$$

$$\beta = l/a \tag{4}$$

J is the overall current density, and F$(\alpha\beta)$ is called the shape factor

Now for a specified central field B_0 and clear bore a, and overall current density is chosen as per the superconductor properties, the shape factor F$(\alpha\beta)$ value can be calculated from (2).

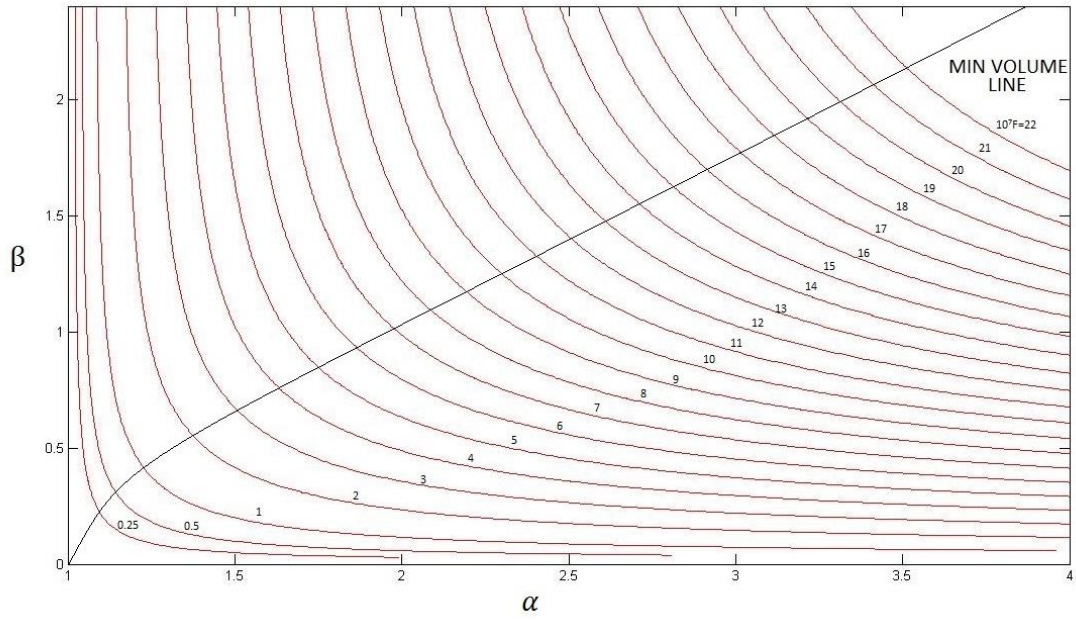

Fig. 2.2 Function F, relating central field with current density, radius and shape factors α *and* β

Fig. 2.2 shows multiple contours of constant F as a function of α and β. Now for any given shape factor we can choose different values of α and β where α gives an indication of the relative length of the magnet compared to clear bore a and β gives an indication of the relative thickness of the magnet compared to clear bore *a.* This indicates that either of a long thin or a short fat coil can be used to obtain the same magnetic field B_0.

The expression for the minimum winding volume is given as, $V = 2\pi a^3(\alpha^2 - 1)\beta$ and is plotted in Fig. 2.2. Now we might think that the combination of α and β that results in minimum winding volume should be chosen, which is not the case, as in doing so we are not taking the effect of α

and β on field uniformity. Field uniformity greatly affects the superconductor's current carrying capacity.

The important thing to notice is that the magnetic field at the center B_0 is not maximum rather the maximum field that the windings are subjected to is B_w as shown in Fig. 2.1. It is this field B_w that decides the critical current density in the windings, hence ideally we would want the ratio B_w/B_o to be minimum so that the superconductor windings are not subjected to fields significantly larger than the useful field B_0. Fig. 2.3 shows some plots of B_w/B_o as a function of α and β . B_w is calculated numerically, as it cannot be calculated analytically.

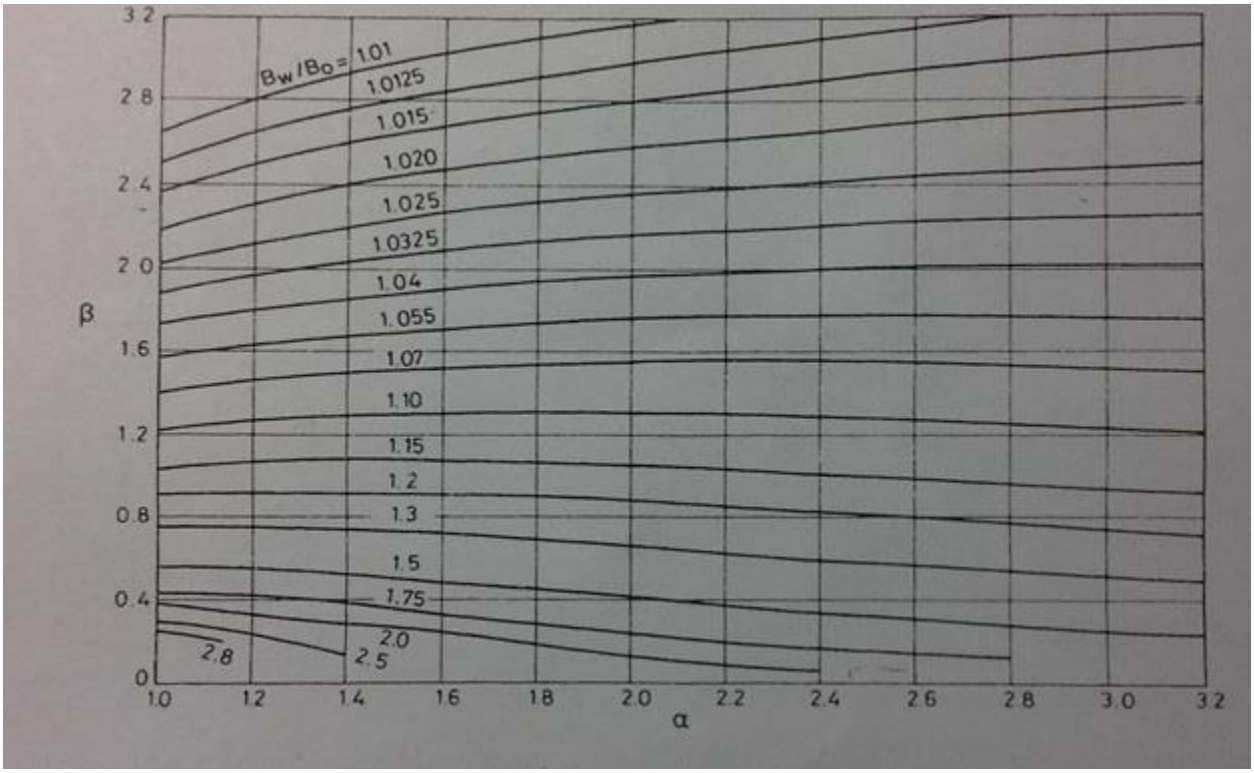

Fig. 2.3 Peak to central field ratio, B_w/B_o in a simple solenoid as a function of the shape factors α and β[1]

An example of a 6T solenoid is considered to better depict the effect that peak field has on the design of the magnet. The upper curve in Fig. 2.4(a) and Fig. 2.4(b) shows critical current density vs. magnetic field at 4.2K for NbTi superconducting material.

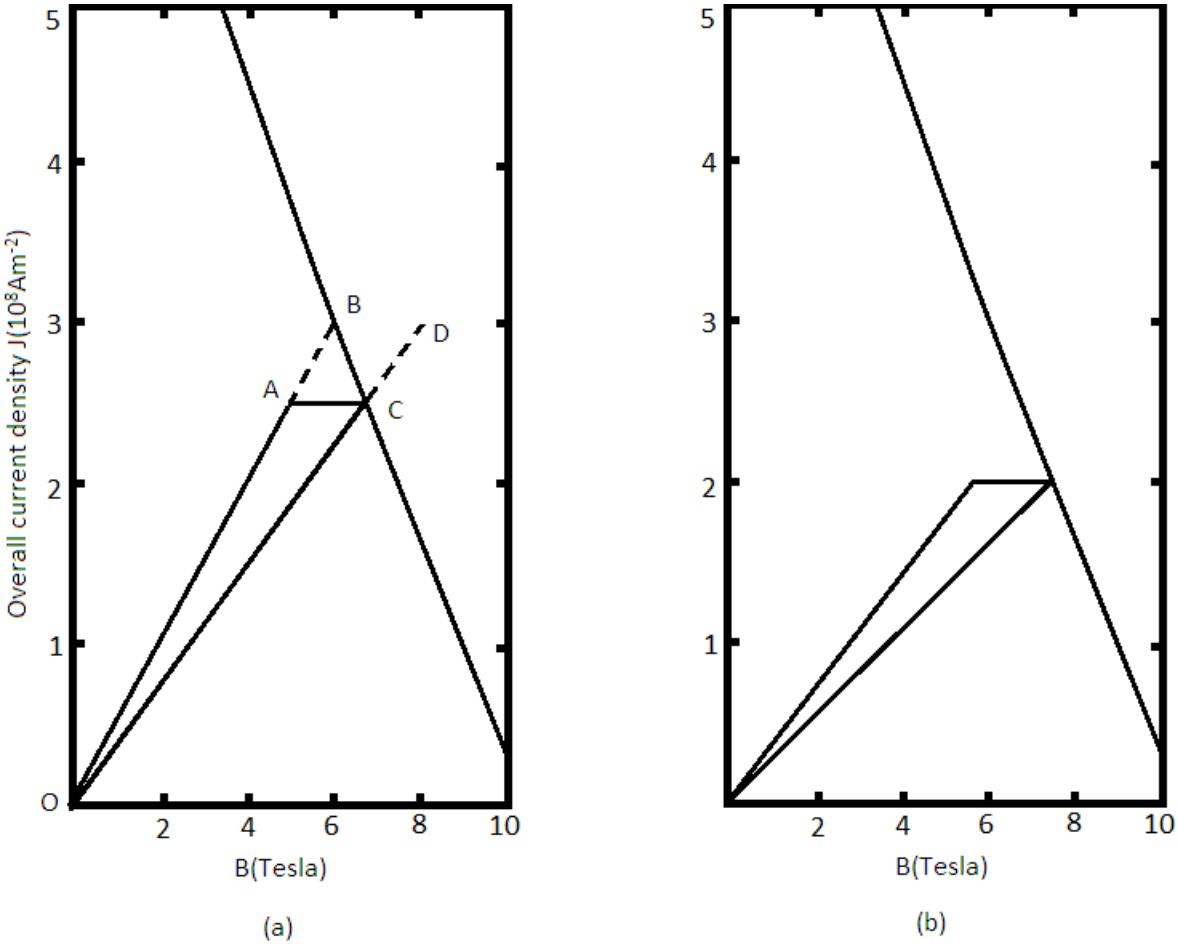

Fig. 2.4 (a) Overall current density of NbTi solenoid with load lines corresponding to maximum and central fields; (b) load lines for production of 6T magnetic field from a winding satisfying minimum volume criterion

Now, as seen from the Fig. 2.4 (a) for 6T the current density required is 3×10^8 Am^{-2}, if peak field is not considered than the magnet coil would need to produce this field at this current density. From (1), F = 2.7×10^{-7}, the contour corresponding to this F value in Fig. 2.2 gives $\alpha = 1.43$

and $\beta = .69$ for minimum volume and from Fig. 2.3 $B_w/B_o = 1.34$, hence we get the new load line OD instead of OB resulting in useful field of only 5T.

But if the ratio B_w/B_o is reduced to 1.25 by having suitable shape factor, for 6T central field peak field will be 7.5T. The corresponding load lines will be as shown in Fig. 2.4 (b) and the working current density for producing 6T central field will be 2×10^{-8} Am^{-2}.

As the magnetic field is different throughout the magnet winding, if the windings are divided into a number of concentric winding sections so that each of these sections can operate at a different maximum current density, decided by the magnetic field they are locally subjected to, which improves the superconductor usage efficiency. This can be done either by having a single current source, but having wires of different diameters for every individual section and connecting them in series so that they operate at different current densities or by having different current sources for each winding section. Generally the former of the two methods is preferred.

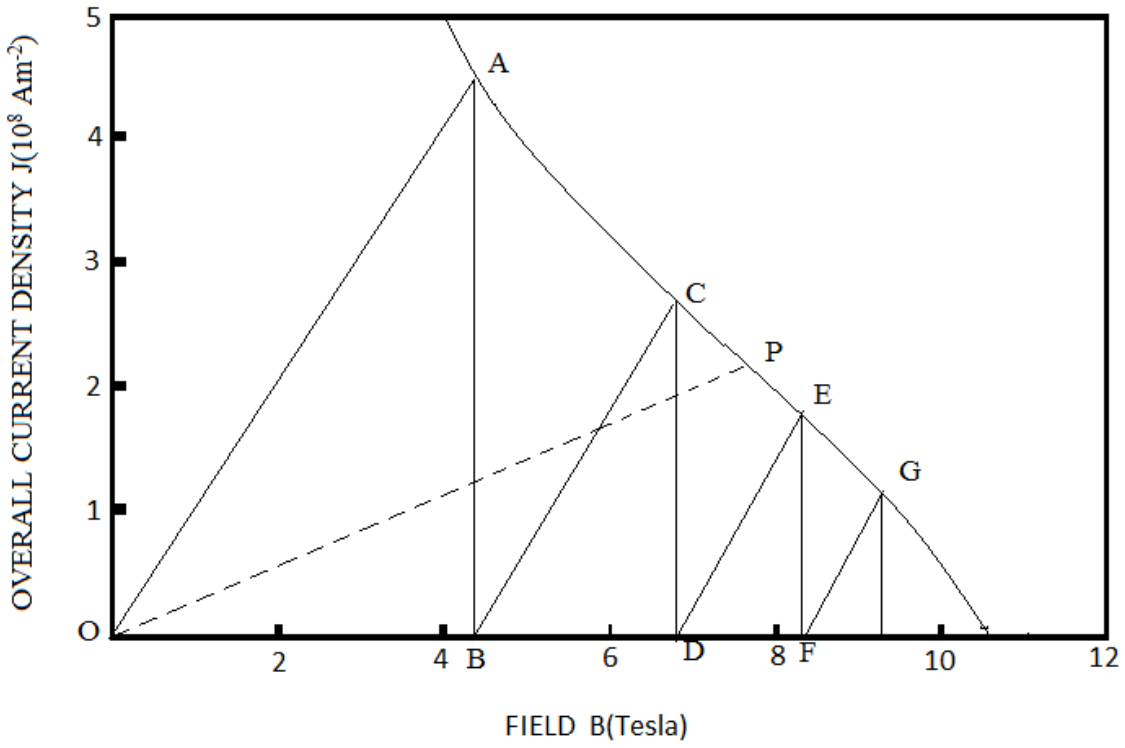

Fig. 2.5 Load lines for a solenoid divided into four section

The impact of dividing the magnet into subsections can be better realized by considering the following example of an ideal long solenoid for which the field remains constant in the axial direction throughout the bore and gradually reduces to zero at the outer winding edge with each section of radial width Δr adds a field of $\Delta B = \mu_0 J \Delta r$ to its bore. Now, assuming each section to be of width 8mm and producing 1T for current density of 4.2×10^8 Am^{-2}. For the outermost section we can draw the load line OA as shown in Fig. 2.5 which gives the critical current density J = 4.2×10^8 Am^{-2} and magnetic field of 4.2T. Now the second section will be in a background magnetic field of 4.2 T and the load line for this section will be BC. Similarly, two more sections can be included so as to get a field of 9.2T at the center. In contrast if we had a single infinitely long solenoid of thickness equivalent to four subsections that is Δr = 32mm, then its slope ΔJ/ΔB will be 4 as shown by the load line OP in the Fig. 2.5 and gives a central field of 7.6 T which is significantly lower than the subdivided case as it does not utilize the available current density at lower magnetic fields to its fullest to get maximum central magnetic field.

One very important aspect of magnet design is the field uniformity obtainable inside the bore of the magnet as most of the leading applications of superconducting magnets include high energy physics experiments like particle accelerators, nuclear magnetic resonance (NMR) etc. which require a uniform magnetic field.

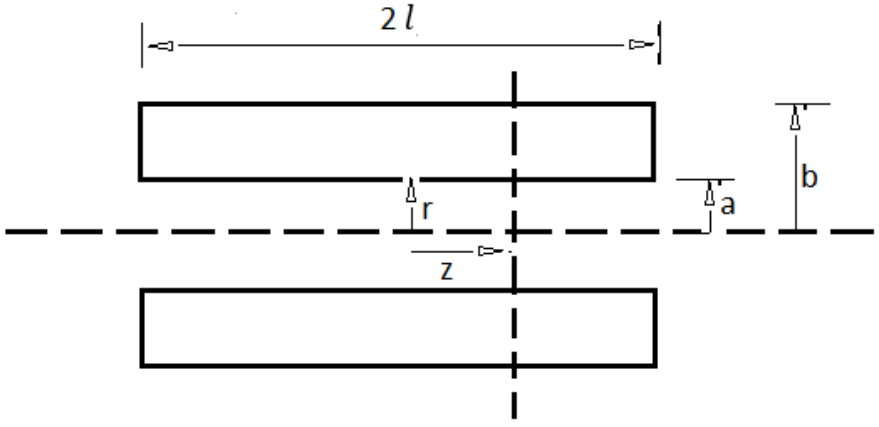

Fig. 2.6 Cross-sectional view of a simple solenoid winding

Now the magnetic field variation along the central axis can be obtained from (1) and (2) by dividing the solenoid in two parts as shown in Fig. 2.6. Field at point z will be

$$B_z = \frac{1}{2} Ja\{\mathrm{F}(\alpha, \beta_1) + \mathrm{F}(\alpha, \beta_2)\}$$

Where,

$$\beta_1 = \frac{(l-z)}{a}, \text{ and } \beta_2 = \frac{(l+z)}{a}$$

At points which are beyond the end of the coil, β_1 or β_2 become negative and

$$\mathrm{F}(\alpha, -\beta) = -\mathrm{F}(\alpha, \beta).$$

By using the properties of electromagnetic fields the following series expansions are written

$$B_z(z,0) = B_0\left\{1 + E_2\left(\frac{z}{a}\right)^2 + E_4\left(\frac{z}{a}\right)^4 + E_6\left(\frac{z}{a}\right)^6 + \cdots\right\} \quad (6)$$

$$B_z(0,r) = B_0\left\{1 - \frac{1}{2}E_2\left(\frac{r}{a}\right)^2 + \frac{3}{8}E_4\left(\frac{r}{a}\right)^4 - \frac{5}{16}E_6\left(\frac{r}{a}\right)^6 + \cdots\right\} \quad (7)$$

Where, E_2, E_4, E_6 are the error coefficients which can be found out as follows

$$E_{2n} = \frac{1}{B_0}\frac{1}{(2n)!}\left.\frac{d^{2n}B_z(z,0)}{dz^{2n}}\right|_{z=0}$$

With proper designing of these error coefficients can be reduced to zero as is done by Helmholtz coil wherein $E_2 = 0$ and notched coils as shown in Fig. 2.7 wherein both E_2 and E_4 can be reduced to zero with proper designing.

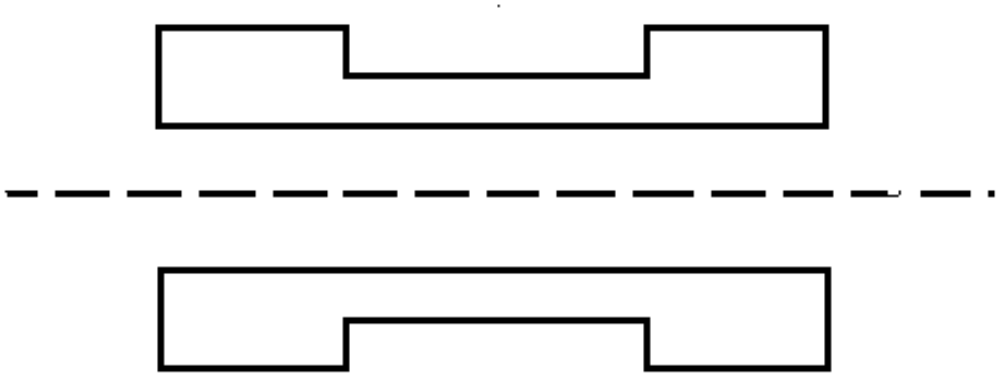

Fig. 2.7 A notched solenoid winding

2.2 Finite element method (FEM) modelling of a simple solenoid and a notched solenoid

Here we are using FEM based software ANSYS Maxwell, which is a high-performance interactive software package based on finite element analysis (FEA) to solve electric, magneto static, eddy current, and transient problems. Finite element refers to the method from which the solution is numerically obtained from an arbitrary geometry by breaking it down into simple pieces called finite elements. These finite elements are triangle for Maxwell 2D and tetrahedron for Maxwell 3D. For a given model the source conditions, boundary conditions, materials of the model must be defined by the user following which Maxwell2D solves the electromagnetic field problems by applying Maxwell's equations over a finite region of space.

A simple solenoid and a notched solenoid with the mentioned design coordinates are modelled using ANSYS Maxwell as shown in Fig 2.8 and Fig. 2.9 below.

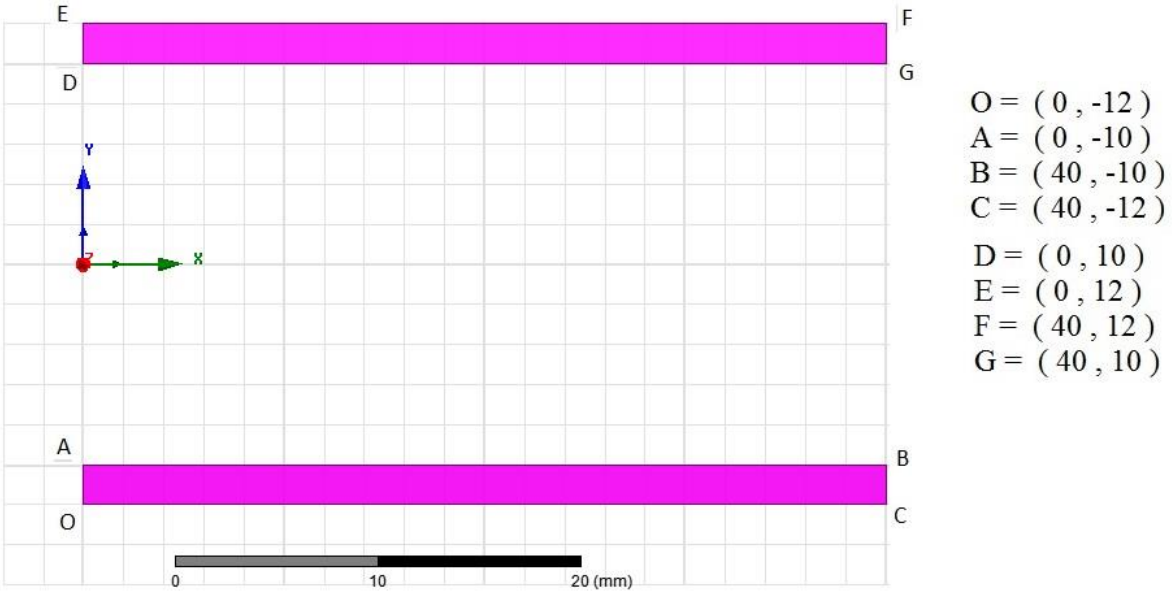

Fig. 2.8 Maxwell model of simple solenoid

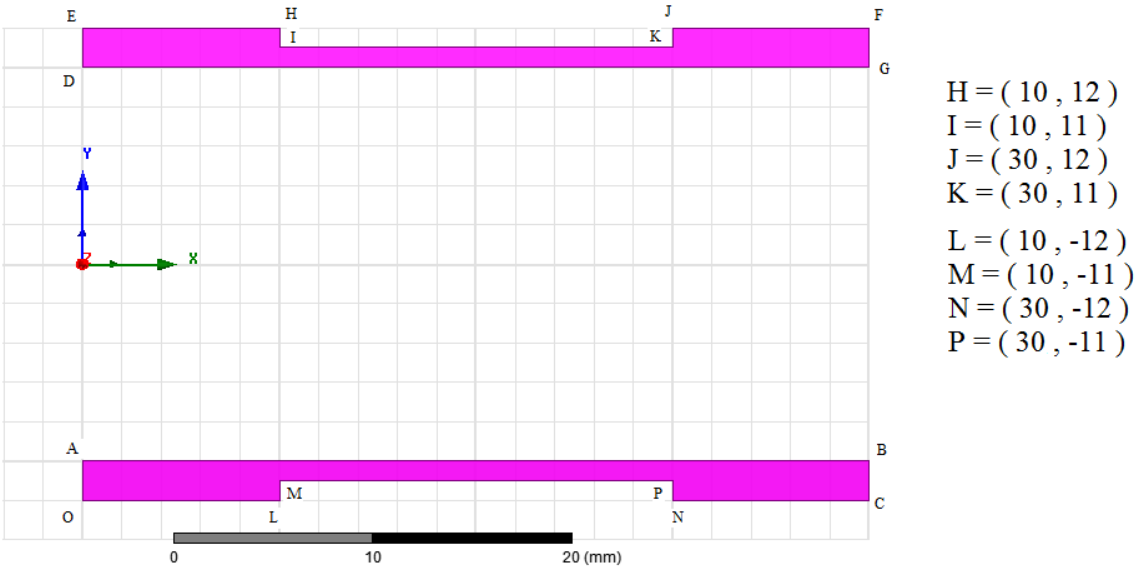

Fig. 2.9 Maxwell model of notched solenoid

The windings are of copper and a current density of $10A/m^2$ is provided as excitation. The magnetic field distribution for both simple solenoid and notched solenoid are plotted as shown in Fig. 2.10 and Fig. 2.11.

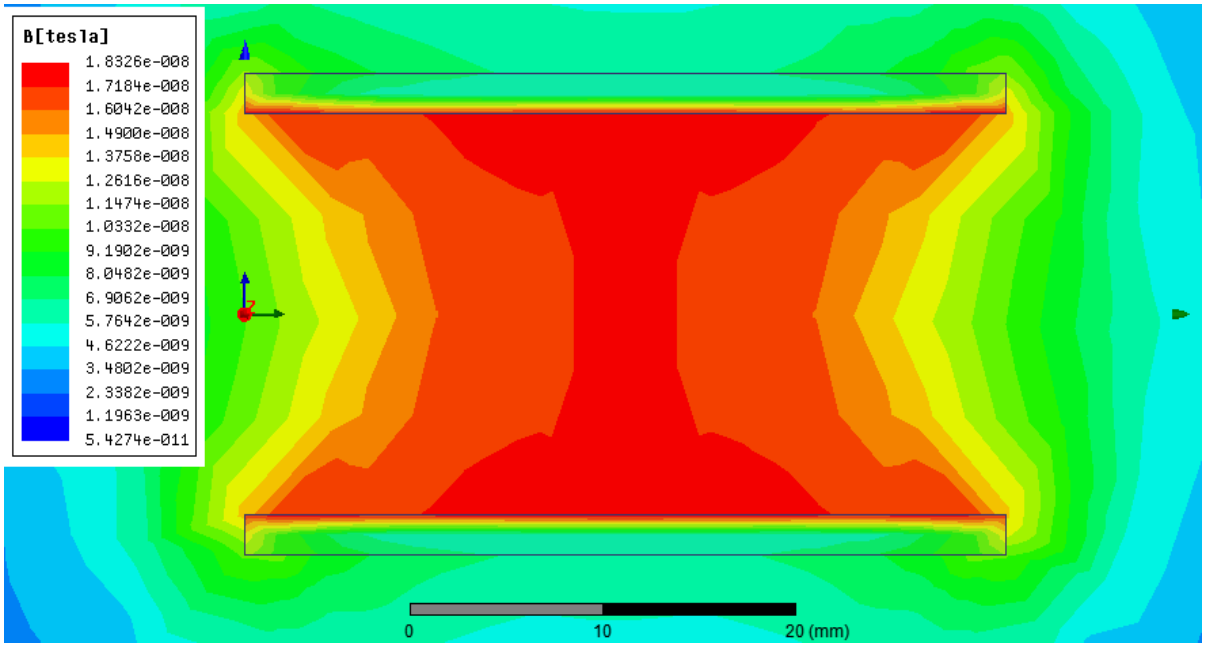

Fig. 2.10 Field density distribution in simple solenoid

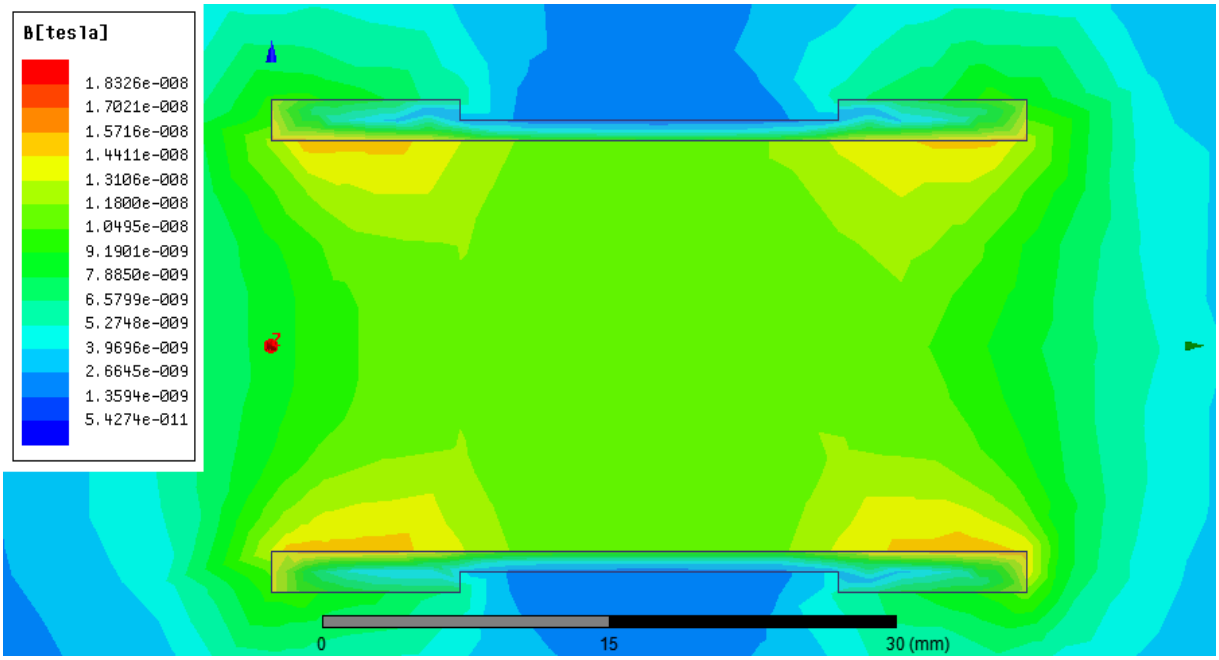

Fig. 2.11 Field density distribution in notched solenoid

It is evidently clear that with notched solenoid the magnetic field distribution inside the bore of the magnet is much more uniformly distributed. To further this point we plot the graph of magnetic field along the central axis for simple solenoid and notched solenoid as shown in Fig 2.12 and Fig 2.13 below.

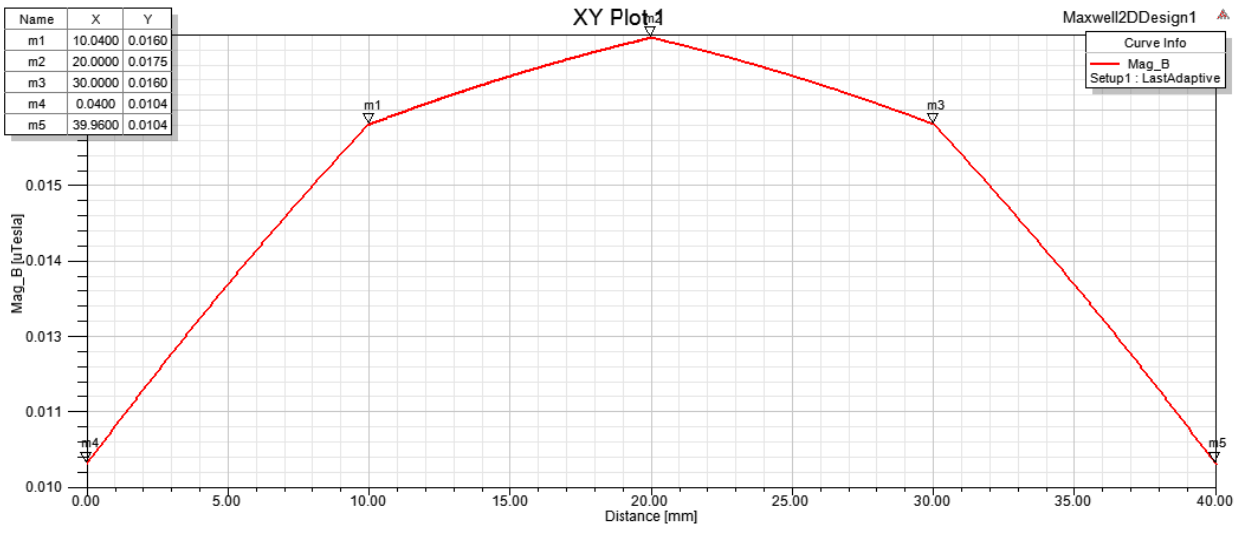

Fig. 2.12 Field density along the central axis of simple solenoid

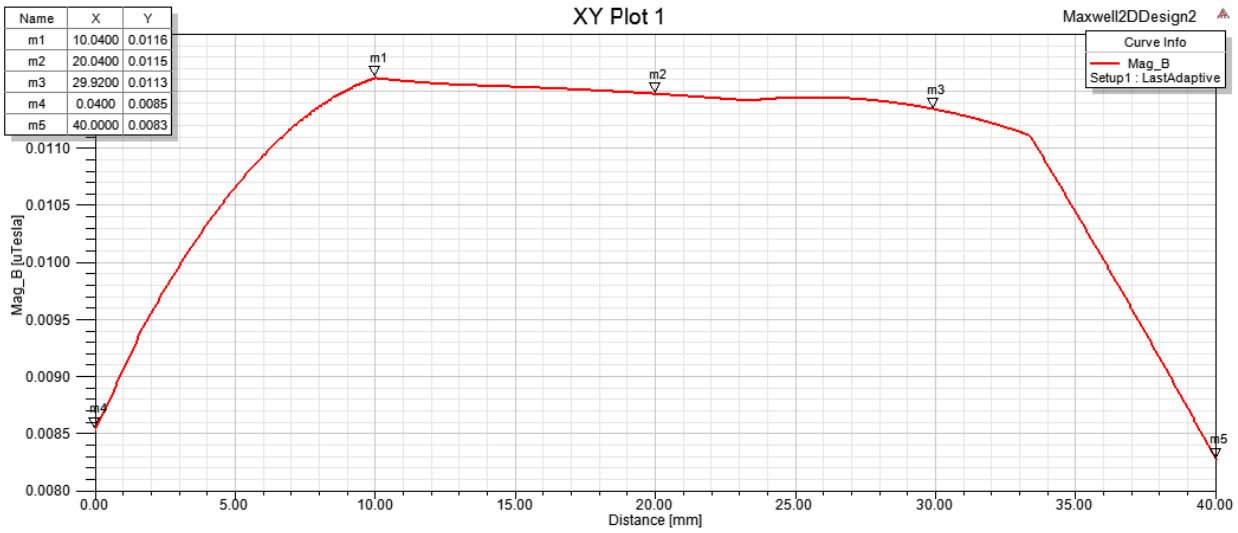

Fig. 2.13 Field density along the central axis of notched solenoid

As expected the magnetic field is much more uniform for notched solenoid, by using compensating winding it can be further improved compared to simple solenoid.

2.3 An example of optimal design of a high magnetic field three section superconducting magnet using genetic algorithm

Super conductor magnet design objective is to obtain minimum volume while satisfying the constraints like thermal stress, Lorentz force, field vs. current density properties of superconductor, homogeneity of magnetic field, protection from quench etc. A three section magnet model with design specifications listed as below is shown in Fig. 2.14.

- 12T central magnetic field,
- an inner bore of radius 5 cm,
- ±0.1T field homogeneity within an area of 2cm radius around the center

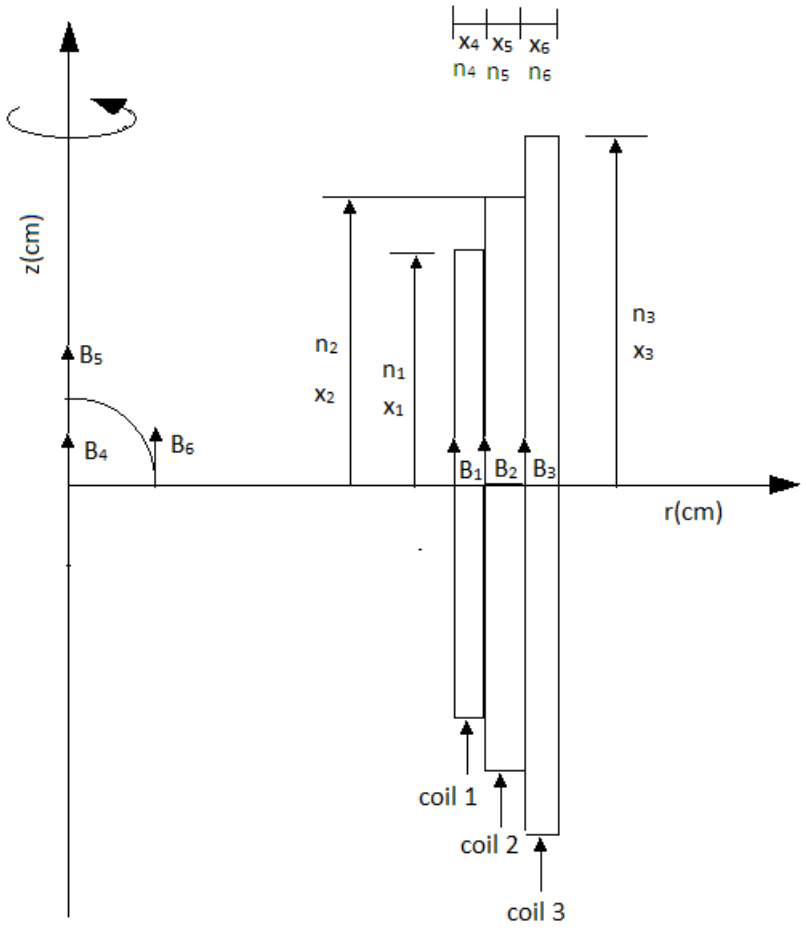

Fig. 2.14 Three section superconducting magnet model

Here x_4, x_5 and x_6 are the individual winding section's thickness, x_1, x_2 and x_3 are half length of coil 1, 2, 3 respectively with magnet's transport current being x_7. B_1, B_2, and B_3 are the maximum field experienced by coil 1, 2 and 3 respectively. B_4, B_5 and B_6 give an indication of magnetic field intensity and homogeneity at the central region. Now the objective function and constraint equations are listed below

$$F = 2\pi\left\{3\left(x_4^2 + 10x_4\right)x_1 + \left(x_5^2 + 2x_4x_5 + 10x_5\right)x_2 + \left(x_6^2 + 2x_4x_6 + 2x_5x_6 + 10x_6\right)x_3\right\} \quad (1)$$

Subjected to

$$11.9 \le B_i \le 12.1 \qquad \text{(i= 4, 5, 6)} \qquad (2)$$

$$x_7 \le -67.6B_1 + 1267.5 \tag{3}$$

$$x_7 \le -203.2B_2 + 2133.6 \tag{4}$$

$$x_7 \le -94.4B_3 + 991.2 \tag{5}$$

Eqn(1) is the objective function or the cost function of the winding subjected to constraint of field homogeneity at the center represented by eqn(2) .eqn(3), (4) and (5) represent the constraint of B-I characteristics of superconductor. Now the above model is optimized by a genetic algorithm whose flow chart is shown in Fig. 2.15.

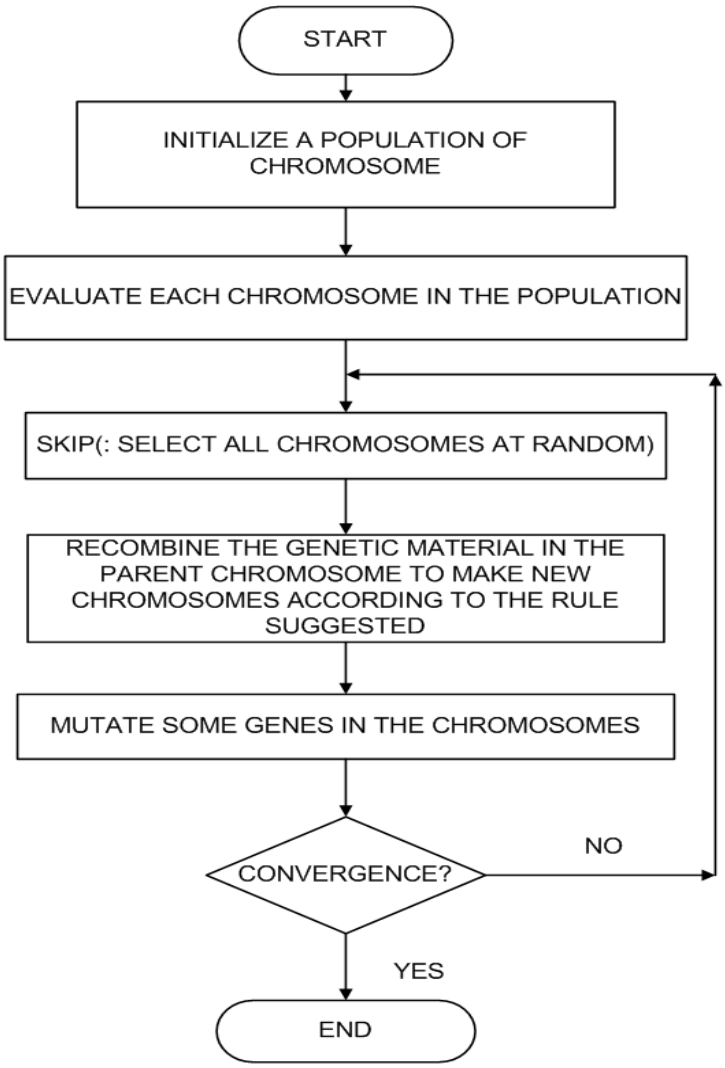

Fig. 2.15 Flowchart of the modified genetic algorithm

CHAPTER 3

Modelling of a 9.2 T NbTi superconducting magnet with long-length uniform axial field

3.1 Introduction

In recent years superconducting magnets have played a pivotal role and proved to be a powerful, reliable and efficient tool in investigation of fundamental phenomenon observed by high energy particles under specified magnetic field [2]. Nuclear magnetic resonance (NMR), is one of the applications of superconducting magnet where a very uniform magnetic field is of essence for the study of resonance of proton [9]. Other applications of superconducting magnet like wiggler and gyrotron require a magnetic field with oscillating or gradient distribution in order to guide the charged particles [10]-[12].

The principal task of the superconducting magnet for gyrotron application is to produce a gradient magnetic field so as to guide the cyclotron electron procession from the cathode to the interaction region along the magnetic line of force. In the interaction region the field is uniform and the emission of coherent electromagnetic radiation at electron cyclotron frequency takes place. Depending on the given application, the cyclotron frequency is a function of electron energy and magnetic field. For example, a 140-160GHz gyrotron oscillator makes use of 4.7~5.8T magnetic field as the interaction field, which is being used as plasma heating in Tokamak fusion experiment [13]-[16].

Superconducting magnets with low magnetic induction have become popular for the high frequency, high power gyrotron users owing to their low cost and for being able to meet the requirements of high frequency experiments with multiple harmonics. The proposed 9.2T superconducting magnet is designed to provide a wide range of frequency experiments capability to the gyrotron users.

3.2 Model description

The predefined design specifications of the 9.2T superconducting magnet are listed below

- A warm bore of 90mm diameter
- An adjustable magnetic field between 0 to 9.2T in the warm hole
- Magnetic field length of at least 200mm length
- Approximate magnetic field of 3000Gs at the cathode

Here the maximum available magnetic field is 9.2T so that we can use NbTi as long as the peak magnetic field that the winding is subjected to stays in the critical surface, meaning that it satisfies the B~I characteristics of NbTi superconducting material. Hence optimization of peak field on the magnet windings becomes an important aspect of magnet design. Fig. 3.1 shows a 3D view of the magnet with its ten co axial coils.

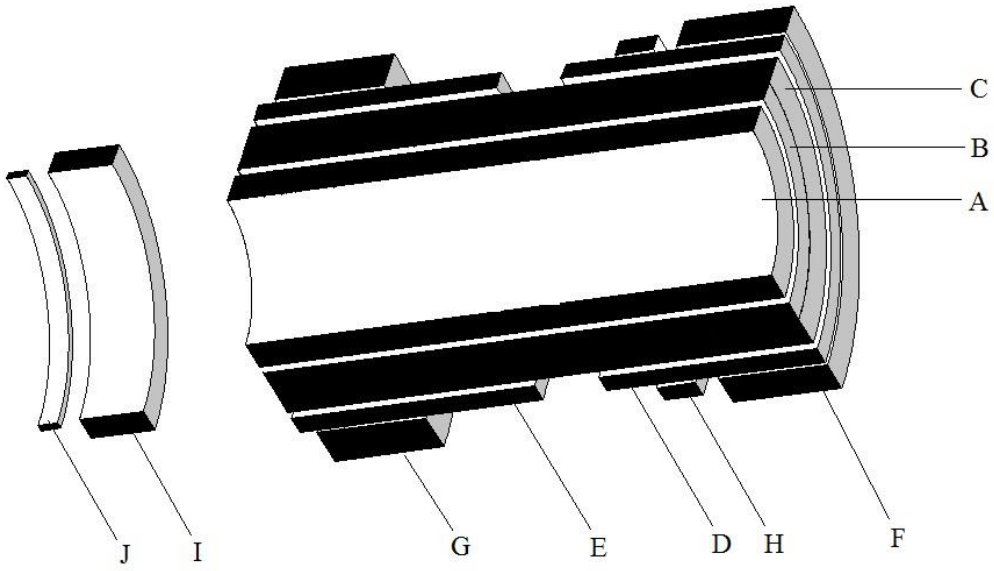

Fig. 3.1 3D view of the magnet coils

As seen from Fig. 3.1 the 9.2T superconducting magnet which consists of 10 individual coaxial coils arranged in different layers and can be subdivided into two parts. The first part being the main magnet, which consist of coil A, B, C, D, E, F, G and H is responsible for the production of specified central magnetic field of 9.2T. The second part consists of coil I and J, also known as the adjusting coils and its function is to restrain the emitted electrons from cathode. The adjusting coils and the main magnet are powered from two different power supplies. Fig. 3.2 shows the cross-sectional view of the superconducting magnet with design specification. The detailed of all the ten coaxial cables are listed in Table.1

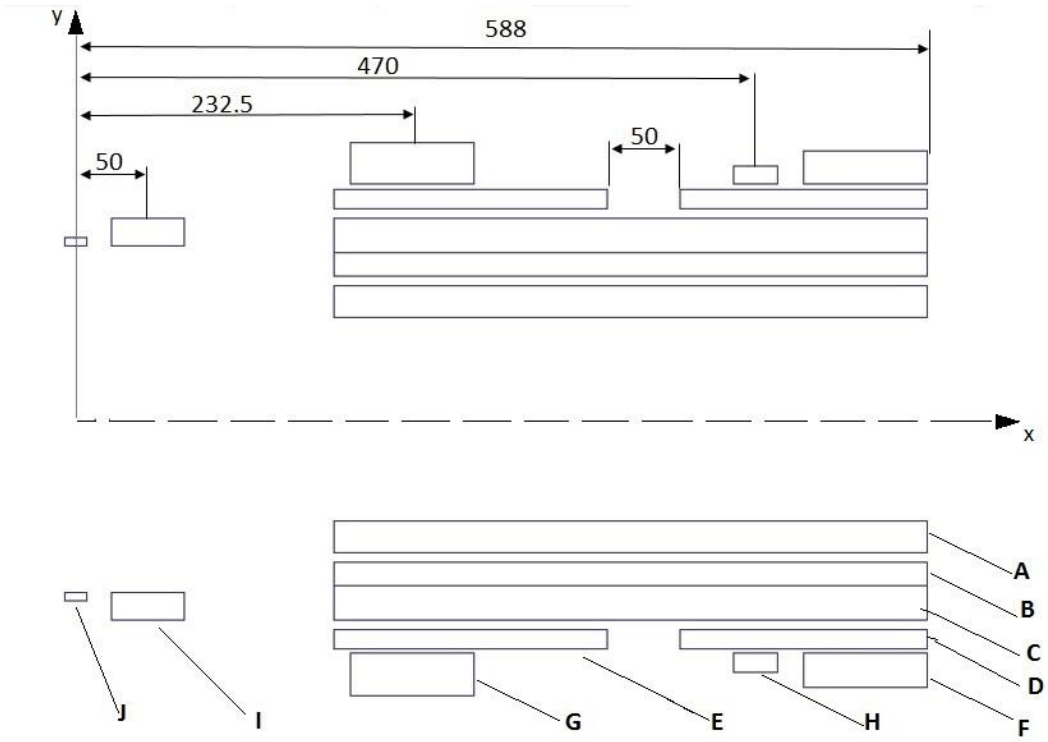

Fig. 3.2 cross-sectional view of the magnet coils

Table 1: Coil Parameters of the magnet

Coil No.	**Inner Diameter**	**Outer Diameter**	**Length(mm)**	**Current Density** $\mathbf{A/mm^2}$
A	140.0	185.0	410.0	68.7
B	198.0	230.0	410.0	85.5
C	230.5	277.5	410.0	108.3
D	290.5	317.9	170.5	229.0
E	290.5	317.9	189.5	181.4
F	323.9	371.3	85.0	229.0
G	323.9	382.1	85.0	229.0
H	323.9	349.8	30.0	229.0
I	240.0	272.5	51.0	229.0
J	240.0	250.8	15.0	229.0

3.3 Simulation results

The 9.2T superconducting magnet is modelled as per the design specifications given in Table.1 and Fig. 3.2 and the magnetic field analysis of the model is performed using Finite Element Method based ANSYS Maxwell simulation kit.

3.3.1 Magnetic field distribution in the magnet model

The magnetic field density magnitude in the magnet model is shown in Fig. 3.3.

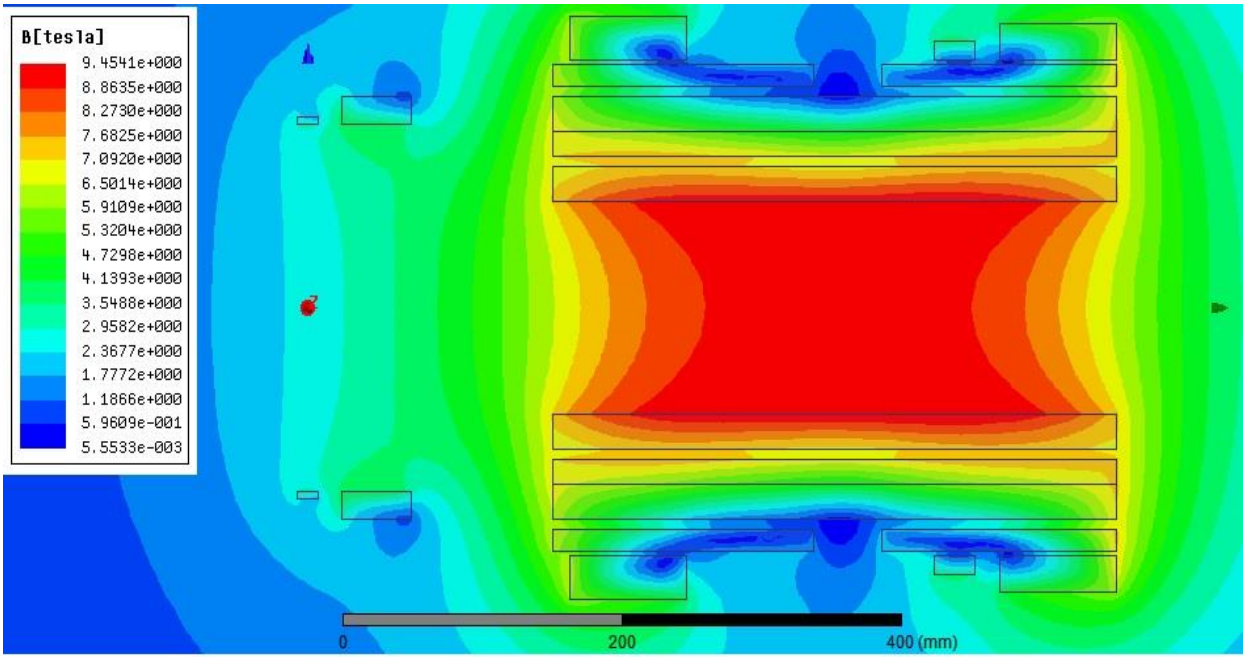

Fig. 3.3 Magnetic field density distribution in the magnet model

A few observations can easily be made by analyzing the magnetic flux density plot in Fig. 3.3. The significantly high degree of uniformity in the magnetic flux density inside the clear bore of the main magnet is evident as compared to a simple solenoid. The magnetic field density is not maximum at the center rather the peak field density is observed at the inner most coil A as pointed out by point m_2 in Fig. 3.4. The peak magnetic field that the coil A, B and C are subjected to is 9.4T, 7.58T, 6.95T respectively as shown in Fig. 3.4. As these coils are subjected to different magnetic fields they can have different current densities by using wires of different diameter, hence improving the superconductor usage efficiency.

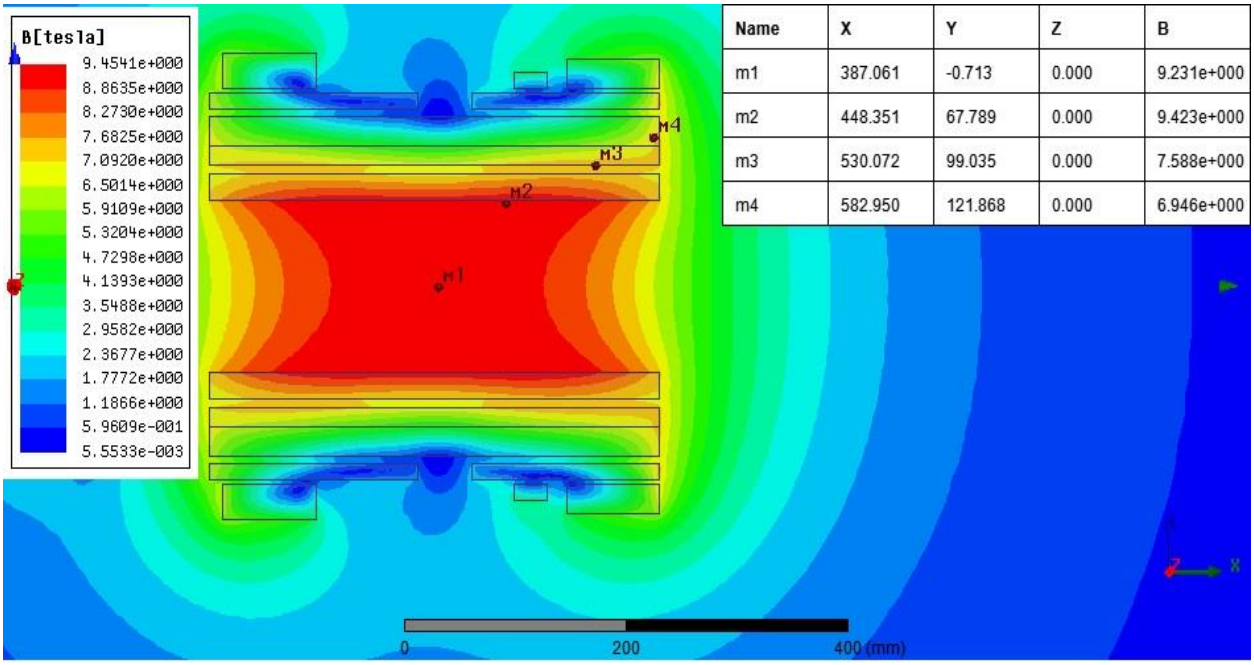

Name	X	Y	Z	B
m1	387.061	-0.713	0.000	9.231e+000
m2	448.351	67.789	0.000	9.423e+000
m3	530.072	99.035	0.000	7.588e+000
m4	582.950	121.868	0.000	6.946e+000

Fig. 3.4 Maximum Magnetic field density distribution in the magnet model winding sections

Now the magnetic field density variation along the central axis of the magnet is plotted in Fig. 3.5

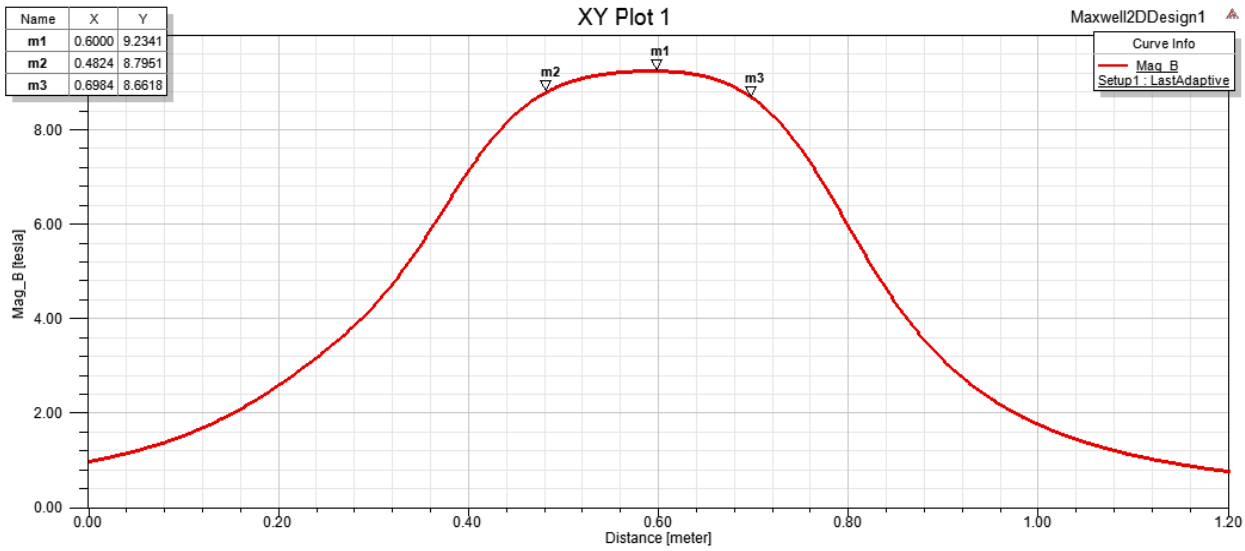

Fig. 3.5 Axial magnetic field distribution in the magnet bore

It is observed that the magnetic field along the central axis has a peak magnetic field of 9.2T and has a high degree of uniformity for an axial length of 150 to 200 mm. the peak field can be regulated by changing the current densities of the coils.

3.3.2 Forces on the coils of the superconducting magnet

There are two kinds of forces acting on the coils of the superconducting. The axial forces and the radial forces. The radial force (also known as hoop stress when stated per unit area) is calculated by doing the cross product between current density J and the axial component of the magnetic field density B_x. Similarly the axial forces on the coils are obtained by doing the cross product between current density J and the radial component of the magnetic field B_y. The axial forces and the radial forces on the windings are shown in Fig. 3.6 and Fig. 3.7 respectively.

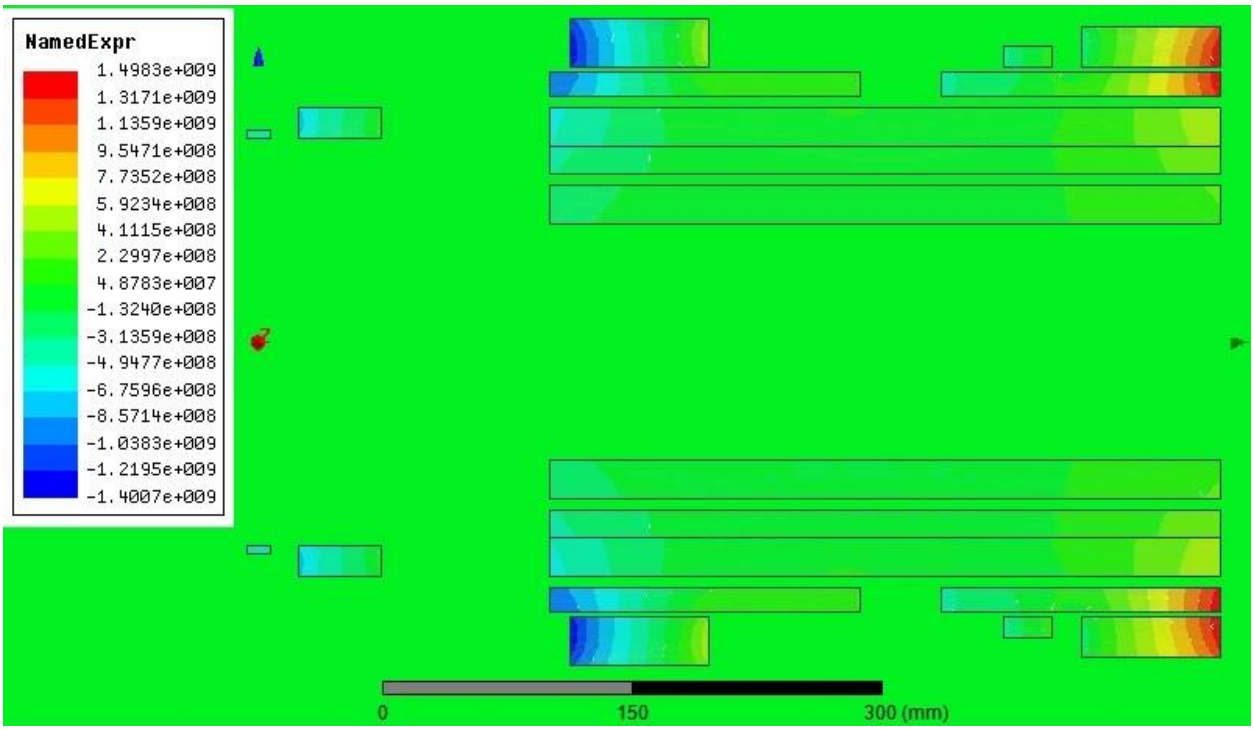

Fig. 3.6 Axial stress on the magnet windings

As seen from Fig. 3.6, the axial force is maximum for coil E and G as the radial component of the magnetic field flux density is maximum for them. Also from Fig. 3.7 it can be seen that the hoop stress is maximum for the innermost windings of coil E and D. Hence while designing the magnet support structure, care is to be taken so that more axial support is provided for coil E and G and

more radial support is provided to coil E and D, in order to bolster up the mechanical integrity of superconducting magnet structure.

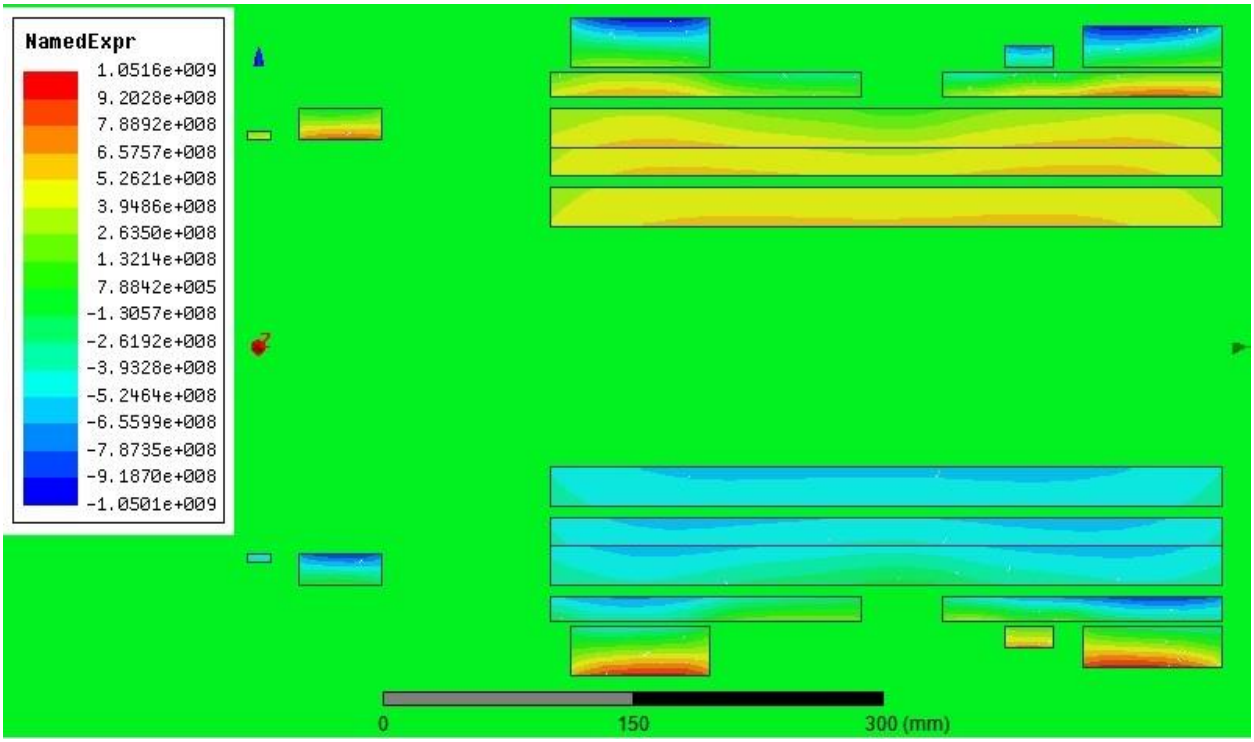

Fig. 3.7 Hoop stress on the magnet windings

CHAPTER 4

Physics of winding deformation

4.1 Introduction

Recent decades have seen a sustained growth in the demand for electrical power, which has led to the creation of more generating capacity and larger number of interconnections between the existing power system networks. The power networks' short circuit capacity has seen a rise because of the above mentioned factors. As a result of this, the power transformers' short circuit duty have become more harsh. Also short circuit faults leading to power transformer failures have become a major concern.

A transformer will be able to withstand the short circuit fault currents and the accompanying short circuit forces caused because of external faults occurrence in the power network, if it has high short circuit strength. Whereas low short circuit strength of the transformer may cause physical collapsing of windings, deformation or damage of the clamping structures, also subsequently might result in electrical faults inside the transformer. These internal faults caused by external short circuit faults pose serious threat as they may cause bursting of tank, blowing out of bushings, fire hazard etc.

4.2 Short circuit forces

Short circuit faults produce large magnitude of currents in the transformer windings. The interaction between this current and leakage flux results in high electromagnetic forces which act on the windings of the transformer. Fig. 4.1 shows the leakage flux between the transformer windings.

The electromagnetic force can be calculated as follows.

$$\boldsymbol{F} = \boldsymbol{L}\,\boldsymbol{I} \times \boldsymbol{B}$$

Here $\boldsymbol{B}$ refers to the magnetic leakage flux density vector, and $\boldsymbol{I}$ refers to the current vector while $\boldsymbol{L}$ refers to the winding length.

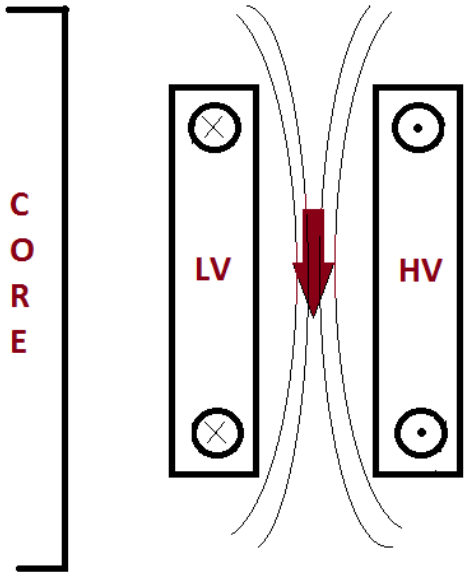

Fig. 4.1 Leakage flux

While analyzing production of electromagnetic forces due to the interaction between current and leakage flux, with the current density vector assumed to be into or out of the paper i.e. in the z direction, the magnetic leakage flux density vector can be divided into two mutually perpendicular components, viz. one in the radial direction ($\boldsymbol{B}_x$) and the second one in the axial direction ($\boldsymbol{B}_y$). Hence, there are mainly two categories of short circuit forces causing the deformation action of the transformer windings, which are axial force defined by expression (2) and radial force defined by expression(3).The action of radial leakage flux density with the current density vector (J) results in axial force (F_y) and can be calculated by eqn(2)

$$F_y = \iint (J \times B_x)\, dx\, dy \tag{2}$$

Similarly, the interaction of axial leakage flux density with current density vector results in radial force (F_x) and can be calculated by eqn(3)

$$F_x = \iint (J \times B_y)\, dx\, dy \tag{3}$$

4.2.1 Radial forces

Radial forces are produced by the interaction of the axial component of leakage flux and the short circuit current flowing in the transformer winding in *z*-direction i.e. perpendicular to the axial leakage field. And the direction of the force can be easily found out using Fleming's left hand rule as shown below in Fig. 4.2. It can be seen from Fig. 4.1 that the axial component of the magnet leakage flux is maximum at the middle portion of the windings, hence the radial force is maximum at this portion too. The axial component of the magnetic leakage flux is diminished at the end of the windings due to fringing effect resulting in lesser radial forces acting at the winding ends.

It can be seen from Fig. 4.2 and verified using Fleming's left hand rule that the radial forces always tend to act outwards on the outer winding, in the process stretching the winding conductors and producing a tensile stress also known as hoop stress. Meanwhile the inner windings are subjected to inward radial force trying to collapse or crush it, hence producing a compressive stress.

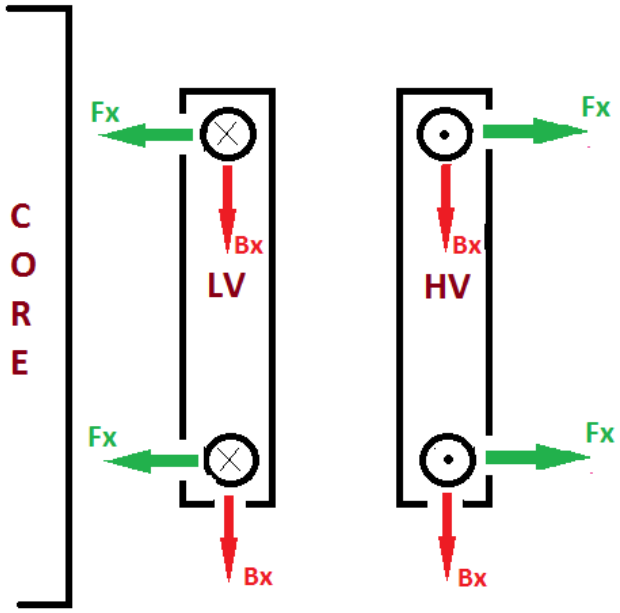

Fig. 4.2 Radial forces on the windings

4.2.2 Axial forces

Axial forces are produced by interaction of the radial component of leakage flux and the short circuit current flowing in the transformer winding in z direction i.e. perpendicular to the radial leakage field. And the direction is found by Fleming's left hand rule as shown in Fig. 4.3. It can be seen that the axial forces at the winding ends are directed towards the winding center for both HV and LV winding.

The radial component of the magnetic leakage flux is maximum at the ends of winding due to fringing effect, hence the local axial force per unit length is maximum at the winding ends but the cumulative compressive axial force is maximum at the center of the windings. Thus for an uniform ampere-turn distribution in windings with equal heights, both the inner and outer windings are subjected to compressive force with no end thrust on the clamping structures.

But if the windings are placed unsymmetrically with respect to the center line, as is shown below

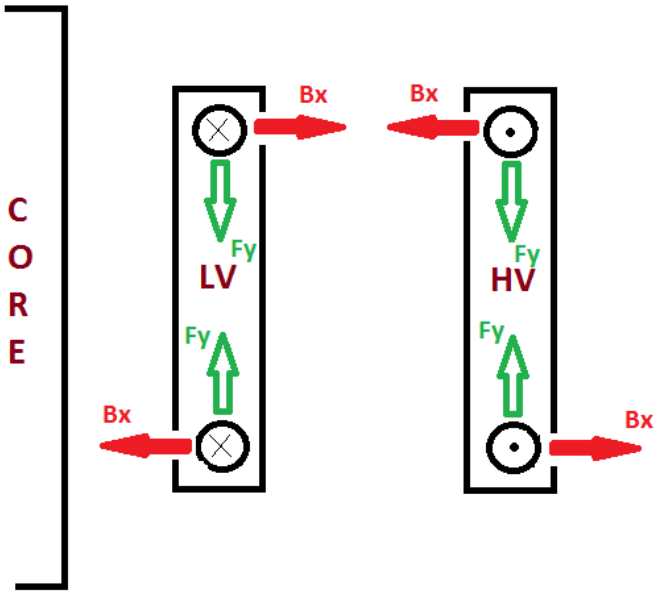

Fig. 4.3 Axial forces on the windings

in Fig. 4.4, the resulting axial forces will act in such a direction so that the end thrusts on the clamping structure and consequently the asymmetry increase further. Hence even a small axial displacement of windings or misalignments of magnetic centers of windings can eventually cause large axial forces leading to failure of transformer.

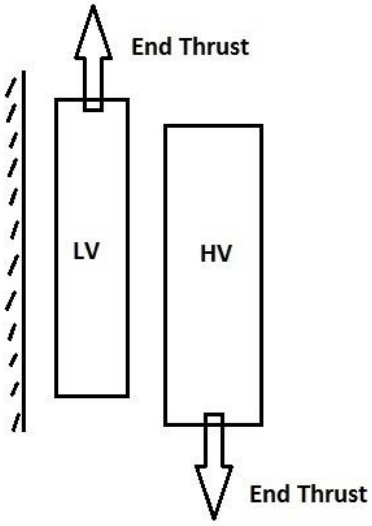

Fig. 4.4 End thrust on windings due to axial asymmetry

4.2.3 Failure modes due to radial forces

The inner and outer windings of transformer are subjected to inward and outward radial forces respectively, hence their failure modes are quite different. The outer winding are subjected to tensile stress (hoop stress) while the inner windings experience a compressive stress. The strength of the outer winding is dependent on the tensile strength of the conductor, meanwhile the strength of the inner winding depends on the support structure provided. Hence the outward bursting of the outer winding is rare, whereas the radial collapse of the inner winding common.

Conductors of inner windings which experience compressive load may fail due to free buckling or forced buckling as shown below in Fig. 4.5 and Fig. 4.6 respectively.

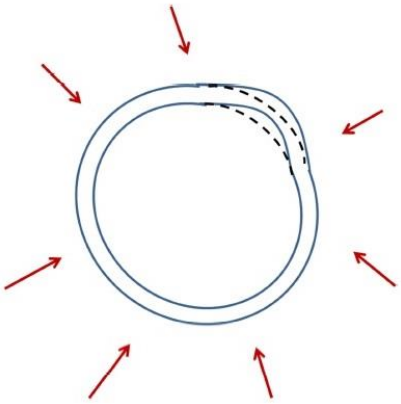

Fig. 4.5 Free buckling

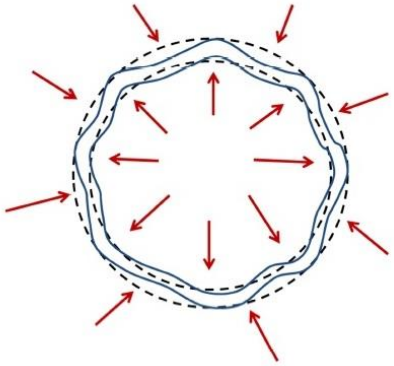

Fig. 4.6 Forced buckling

4.2.4 Failure modes due to axial forces

The various types of failures under the action of axial compressive forces include

- Bending between radial spacers
- Conductor tilting
- Displacement of the complete winding
- Axial overlap of conductors

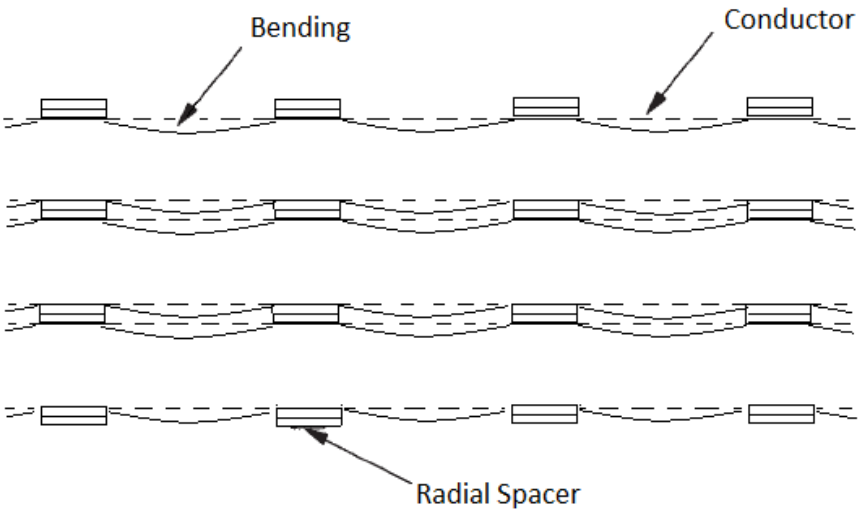

Fig. 4.7 Bending between radial spacers

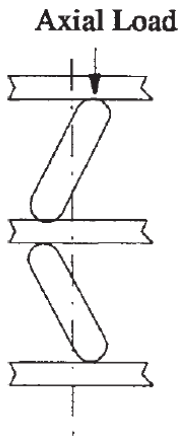

Fig. 4.8 Conductor tilting in a disk winding

4.3 Finite element method (FEM) modelling of a transformer

A transformer with design specification as given in Table 2 is modeled in FEM based software ANSYS Maxwell as shown in Fig. 4.9. The material used for core is steel, copper for the winding and the whole model is enclosed in a region of air which acts as boundary. At normal operating condition of transformer and if the windings are placed symmetrically with respect to the center line, both primary and secondary windings will have rated current flowing through them. But if

due to any mismatch of height of windings an asymmetry is created then high end thrust is produced at the ends of the winding in a direction so as to further the asymmetry.

Table 2: Design specifications

Winding	Inner radius(mm)	Outer radius(mm)	Height(mm)	Turns	Rated current(A)
LV winding	306.5	388	1136	10	2100
HV winding	413	510.5	1136	60	350

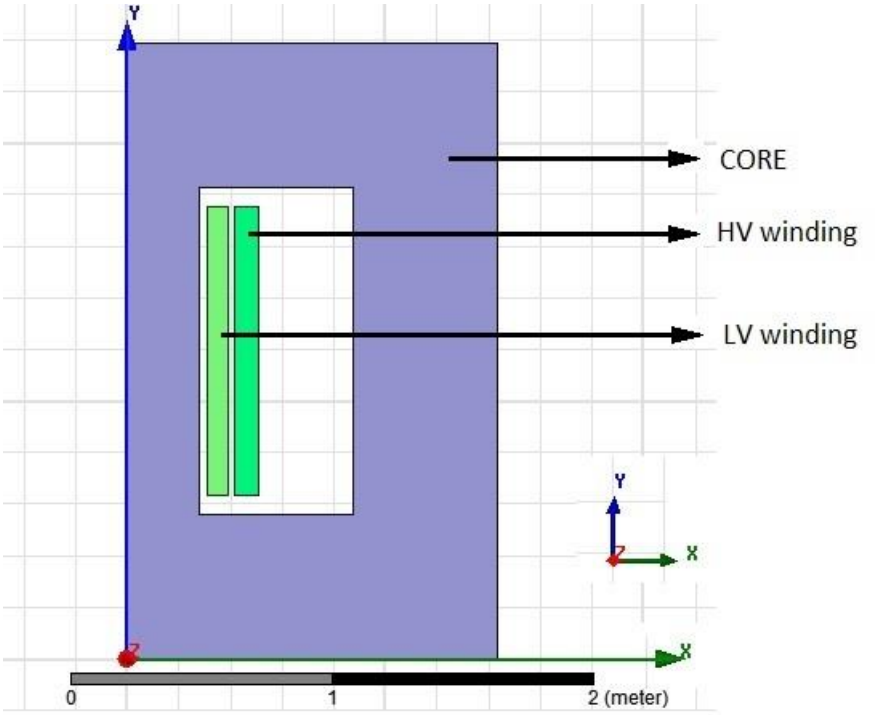

Fig. 4.9 Cross-sectional view of the FEM modelled transformer

4.3.1 Simulation results

Simulation of the above model is done using FEM based software kit ANSYS Maxwell, and the flux pattern, and the shaded plot of magnetic flux density is shown in Fig. 4.10 and Fig. 4.11 respectively. It can be observed that the magnetic field flux density is maximum between the windings discernible by the dark red zone in Fig. 4.11.

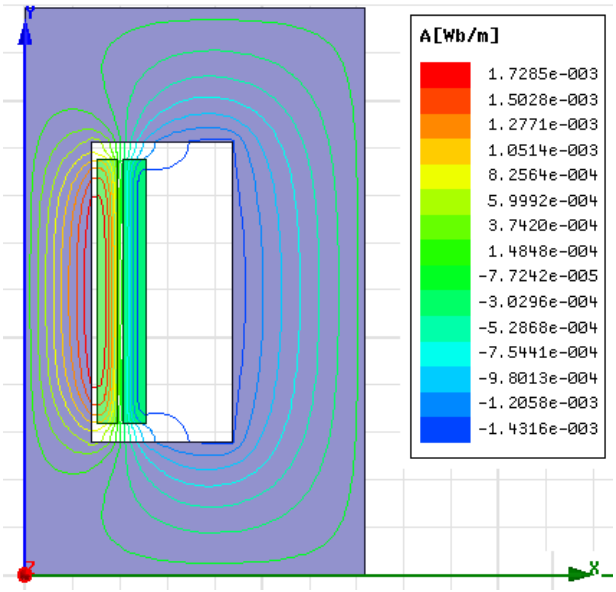

Fig. 4.10 Flux pattern

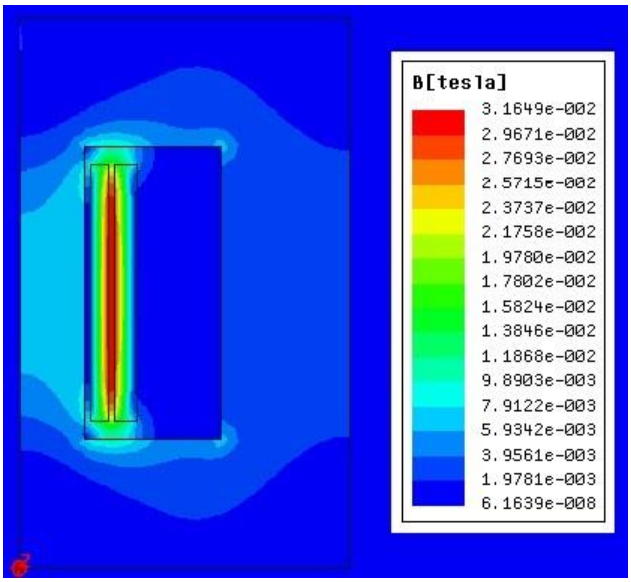

Fig. 4.11 Shaded plot of magnetic flux density

Now an axial asymmetry is introduced and comparison of radial forces, axial forces is done and the corresponding plots are shown below.

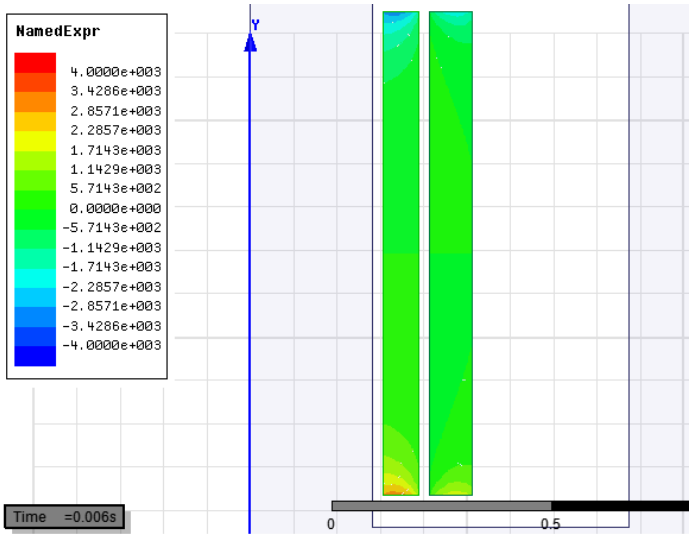

Fig. 4.12 Axial force distribution for symmetric winding

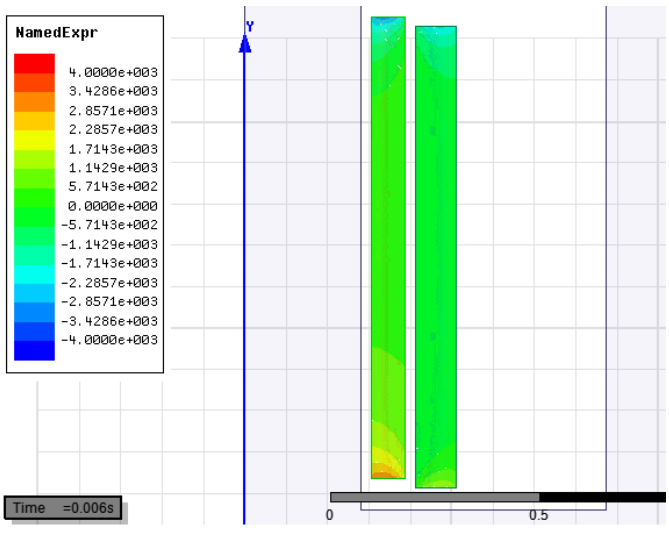

Fig. 4.13 Axial force distribution for asymmetric winding

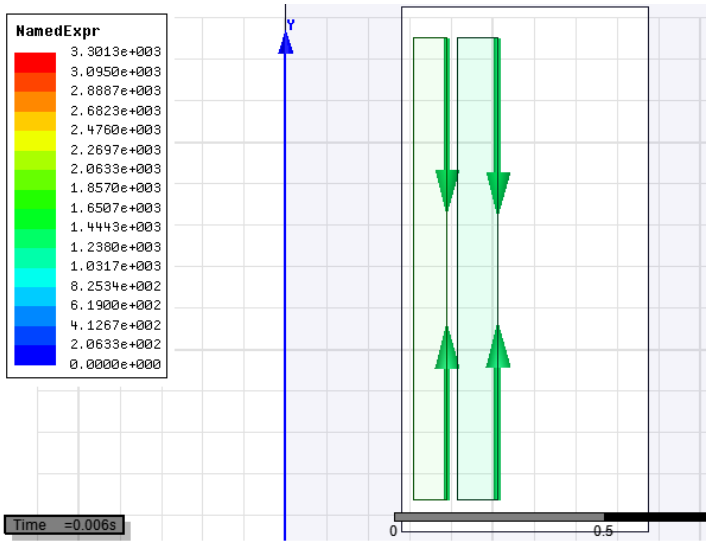

Fig. 4.14 Axial force vector for symmetric winding

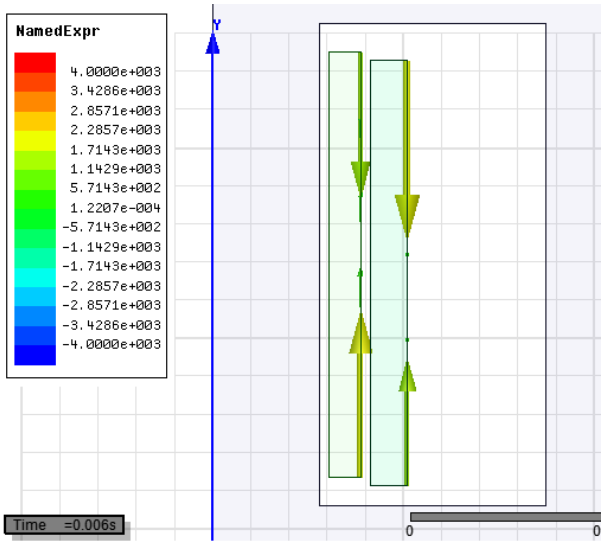

Fig. 4.15 Axial force vector for asymmetric winding

As an asymmetry is introduced it can be seen that the axial forces acting on the winding have increased significantly and the net force acting on them are such that they tend to increase the asymmetry. Meanwhile the radial forces on the windings are not much affected by this as can be seen in Fig. 4.16 and Fig. 4.17 below.

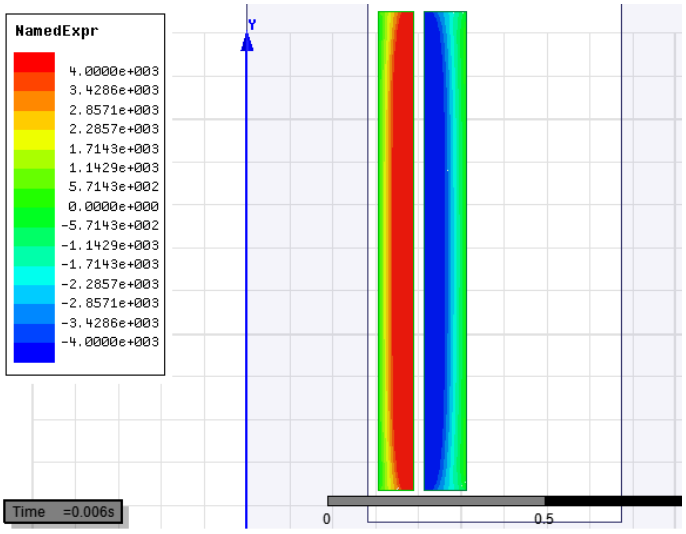

Fig. 4.16 Radial force distribution for symmetric winding

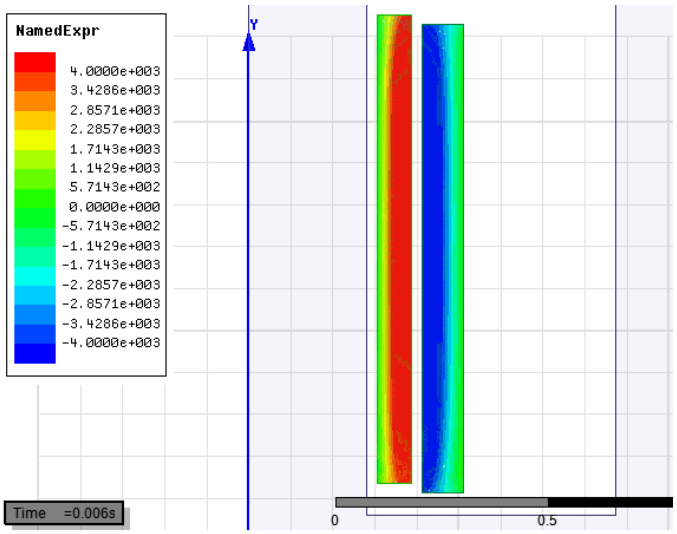

Fig. 4.17 Radial force distribution for asymmetric winding

CHAPTER 5

SUMMARY AND WORKDONE

5.1 Summary and work done

A simple solenoid winding and a notched solenoid winding are designed and modelled using finite element method (FEM) based software ANSYS Maxwell. It is shown that with a notched solenoid winding we are able to get a more uniform magnetic field over the axial length of the magnet bore compared to simple solenoid winding.

A superconducting magnet design consisting of ten coaxial coils is modelled using ANSYS Maxwell in order to obtain a central magnetic field of 9.2T which can be varied in the range of 0 to 9.2T by varying the current density in the coils. Also a uniform axial field is obtained over a long length (Approximately 200mm). Maximum magnetic field for each winding is observed so that their individual current densities can be set to be maximum and inside the critical surface of the superconducting material in order to improve the super conductor usage efficiency. Also hoop stress and axial stress on the windings are calculated and plotted using the field calculator of ANSYS Maxwell, so that mechanical strength of magnet structure can be bolstered up by providing proper radial and axial support to the windings.

Also a transformer design is modelled using ANSYS Maxwell and a small axial asymmetry is introduced between the LV and HV winding, subsequently variation of magnetic field, flux lines, axial and radial force distribution on both LV and HV windings are plotted and found to be in accordance with the theoretical concepts.

5.2 Future work

- Techniques like genetic algorithm can be implemented to get optimal magnet configuration with minimum winding volume.
- In this thesis, notched solenoid magnet design is modelled using FEM modelling approach to get more uniform axial field then simple solenoid winding, similarly magnet with ten coaxial coils is modelled for a long uniform axial field, and these designs can be practically implemented.

References

[1] Martin N. Wilson, “Superconducting Magnets”, Clarendon Press, 1987

[2] Yinming Dai; Hui Wang; Xinning Hu; Shunzhong Chen; Junsheng Cheng; Chunyan Cui; Housheng Wang; Baozhi Zhao; Yi Li; Luguang Yan; Qiuliang Wang, "Design Study on a 9.2-T NbTi Superconducting Magnet With Long-Length Uniform Axial Field," *Applied Superconductivity, IEEE Transactions on* , vol.25, no.3, pp.1-4, June 2015

[3] Noguchi, S.; Ishiyama, A., "An optimal design method for high-field superconducting magnets with ferromagnetic shields," *Applied Superconductivity, IEEE Transactions on* , vol.7, no.2, pp.439-442, June 1997

[4] Noguchi, S.; Ishiyama, A., "An optimal design method for highly homogeneous and high-field superconducting magnets," *Magnetics, IEEE Transactions on* , vol.32, no.4, pp.2655-2658, Jul 1996

[5] Hao Xu; Conolly, S.M.; Scott, G.C.; Macovski, A., "Homogeneous magnet design using linear programming," *Magnetics, IEEE Transactions on* , vol.36, no.2, pp.476-483, Mar 2000

[6] Salon, S.; Lamattina, B.; Sivasubramaniam, K., "Comparison of assumptions in computation of short circuit forces in transformers," *Magnetics, IEEE Transactions on* , vol.36, no.5, pp.3521-3523, Sep 2000.

[7] Tang Yun-Qiu; Qiao Jing-Qiu; Xu Zi-Hong, "Numerical calculation of short circuit electromagnetic forces on the transformer winding," *Magnetics, IEEE Transactions on* , vol.26, no.2, pp.1039-1041, Mar 1990.

[8] S. V. Kulkarni, and S. A. Khaparde, “Transformer Engineering Design and Practice”, New York: Marcel Dekker, 2004.

[9] H. J. Schneider-Muntau, “High field NMR magnets,” *Solid State Nucl. Magn. Reson.,* vol. 9, no. 1, pp. 61–71, Nov. 1997.

[10] E. B. Blum *et al.*, “A superconducting wiggler magnet for the NSLS x-ray ring,” in *Proc. Part. Accel. Conf.*, 1997, vol. 3, pp. 3494–3496.

[11] V. A. Flyagin, A. V. Gaponov, M. I. Petelin, and V. K. Yulpatov, “The gyrotron,” *IEEE Trans. Microw. Theory Techn.*, vol. MTT-25, no. 6, pp. 514–521, Jun. 1977.

[12] C. Du and P. Liu, *Millimeter-Wave Gyrotron Traveling-Wave Tube Amplifiers*. Berlin, Germany: Springer-Verlag, 2014, pp. 4–10.

[13] X. Donghui *et al.*, "The 5.8 T cryogen-free Gyrotron superconducting magnet system on HL- 2A," *Plasma Sci. Technol.*, vol. 16, no. 4, pp. 410–414, Apr. 2014.

[14] J.-P. Hogge *et al.*, "Development of a 2-MW, CW coaxial gyrotron at 170 GHz and test facility for ITER," *J. Phys., Conf. Ser.*, vol. 25, no. 1, pp. 33–44, 2005.

[15] K. Felch *et al.*, "Recent ITER-relevant gyrotron tests," *J. Phys., Conf. Ser.*, vol. 25, pp. 13–23, 2005.

[16] R. Hirose *et al.*, "Development of 7 T cryogen-free superconducting magnet for gyrotron," *IEEE Trans. Appl. Supercond.*, vol. 18, no. 2, pp. 920–923, Jun. 2008.

List of Publications

[1] Kumar Patel, A.; George, N.; Gopalakrishna, S.; Sahoo, S.K., "Optimal high frequency model for analysis of winding deformation in power transformers," *Signal Processing, Informatics, Communication and Energy Systems (SPICES), 2015 IEEE International Conference on* , vol., no., pp.1,5, 19-21 Feb. 2015.